Antidepressants are complex regulators of lipoprotein(a) macropinocytosis.

Gregory MI Redpath[1,2]*, Nikita Deo[1,2]*, Halima Siddiqui[1,2], Golnoush Madani[1.2], Natasha Kapoor-Kaushik[3], Nicholas Ariotti[3], Malcolm Rutledge[1,2], Michael Williams[2,4], Sally PA McCormick[1,2].

*These authors contributed equally to this work.

***Affiliations**:*

[1] Department of Biochemistry, University of Otago, Dunedin, New Zealand.
[2] HeartOtago, University of Otago, Dunedin, New Zealand.
[3] Electron Microscopy Unit, Mark Wainwright Analytical Centre, University of New South Wales, NSW, Sydney, Australia.
[4] Department of Medicine, Dunedin School of Medicine, University of Otago, Dunedin, New Zealand.

***Corresponding author**:*

Professor Sally PA McCormick
Correspondence: sally.mccormick@otago.ac.nz

Summary *(150w)*

Elevated lipoprotein(a) (Lp(a)) levels are an important independent risk factor for developing cardiovascular disease (CVD). Efforts to effectively reduce Lp(a) levels in circulation have been hampered due to a limited understanding of its cellular metabolism. Our data shows that Lp(a) uptake is mediated by the fluid-phase endocytic process, macropinocytosis. Interestingly, commonly prescribed antidepressants can differentially modulate Lp(a) macropinocytosis *in vitro*, increasing Lp(a) uptake in liver cells while decreasing it in macrophages. Our finding that Lp(a) is internalised by macropinocytosis represents a major paradigm shift in Lp(a) biology, potentially reconciling the often contradictory and incongruous studies investigating receptor-mediated Lp(a) uptake.

Abstract

The regulation of Lp(a) clearance from circulation by cellular uptake remains enigmatic. While multiple receptors have been implicated in Lp(a) uptake, each receptor only partially accounts for this uptake, and no endocytic mechanism has yet been prescribed for Lp(a) internalisation into the cell. In this study, we define macropinocytosis as the endocytic pathway responsible for internalising Lp(a). In both liver and macrophage cells, Lp(a) uptake is dependent on extracellular calcium and is inhibited by amiloride or its derivative EIPA. The uptake of apo(a) alone is mediated by macropinocytosis, indicating the apo(a) protein component is a primary regulator of Lp(a) uptake. Importantly, we found that common antidepressants modulate Lp(a) macropinocytosis in cell-type dependent manners. In macrophages, the tricyclic antidepressant, imipramine and selective serotonin reuptake inhibitors (SSRIs) citalopram, fluoxetine and sertraline all inhibit Lp(a) uptake. In liver cells, imipramine and citalopram strongly stimulated Lp(a) uptake, while sertraline inhibited uptake. Imipramine and citalopram enhanced Lp(a) uptake by enhancing cell surface binding of Lp(a) rather than upregulating macropinocytosis *per se*, indicating that immobilisation of Lp(a) on the plasma membrane is an important regulatory step in Lp(a) macropinocytosis. As the liver is the major catabolic route for Lp(a), we dissected the functional consequences of imipramine and citalopram stimulated uptake in liver cells. Both drugs increased Lp(a) delivery to Rab11-positive recycling endosomes, but not late

endosomes or lysosomes, resulting in increased apo(a) recycling into the cellular media. Given that free apo(a) is reported to undergo consistent proteolysis in the extracellular space or in circulation, these results support the potential for the already approved drugs, imipramine and citalopram, as promising therapeutics to lower Lp(a) levels. This approach displays special utility in the large group of people who suffer from depression and anxiety for whom these drugs are commonly prescribed.

Keywords

lipoprotein(a), macropinocytosis, intracellular trafficking, atherosclerosis, selective serotonin reuptake inhibitors, Rab11, depression, endocytosis, citalopram, imipramine.

Introduction

Lipoprotein(a) (Lp(a)) is a highly atherogenic form of low-density lipoprotein (LDL) (Boerwinkle et al., 1992). Lp(a) consists of an LDL-like particle containing apolipoprotein-B (apoB), covalently bound to apolipoprotein(a) (apo(a)), a glycoprotein that is structurally similar to plasminogen (Lawn et al., 1997). Lp(a) is elevated (greater than 100 nmol in at least 20% of the population (Wilson et al., 2019) and recent data from the United Kingdom Biobank indicates that every 50 nmol increment increase in Lp(a) imparts a greater risk of cardiovascular disease (CVD) development (Patel et al., 2020). While LDL is often referred to as the “bad” cholesterol, elevated Lp(a) levels are frequently overlooked despite having an equal impact on CVD development and risk (Langsted and Nordestgaard, 2020). Unlike with LDL, specific Lp(a) lowering treatments remain limited, with RNA antisense therapy targeted to apo(a) being the only treatment close to becoming clinically available (Lippi et al., 2020). Understanding how LDL is cleared from circulation by endocytosis has led to the development of new therapies such as PCSK9 inhibitors (Chaudhary et al., 2017) to lower LDL. Despite the importance of endocytic processes in lipoprotein clearance, little is known about the endocytic regulation of Lp(a). The inability to ascribe a clear single receptor that mediates Lp(a) uptake has hampered the development of effective therapies for Lp(a) lowering.

Multiple receptors have been implicated in binding Lp(a) and mediating Lp(a) endocytic uptake into the cell including the LDL receptor (Floren et al., 1981; Hofmann et al., 1990; Romagnuolo et al., 2017; Tam et al., 1996) , VLDL receptor (Argraves et al., 1997) and plasminogen receptors (Sharma et al., 2017), yet in each case the impact of each receptor on Lp(a) uptake is either inconsistent or only partially responsible for uptake, leaving our understanding of the process of Lp(a) catabolism incomplete (Chemello et al., 2020; McCormick and Schneider, 2019; Rader et al., 1995; Reblin et al., 1997; Romagnuolo et al., 2017). Genome-wide association studies have revealed associations between Lp(a) levels and single nucleotide polymorphisms in genes coding for regulators of endocytic processes such as SNX9 and apoE (Lu et al., 2015; Mack et al., 2017). These data strongly suggest that endocytic processes play a central role in driving Lp(a) catabolism, yet the receptors, ligands and precise endocytic process mediating the uptake has not been explored. Given the multitude of receptors implicated in Lp(a) uptake without any clearly defined role in Lp(a) endocytosis, we hypothesised that Lp(a) uptake occurs *via* the endocytic process called macropinocytosis.

There are many pathways of endocytosis identified to date, each with specific cargoes, activation conditions and functions (Redpath et al., 2020). Clathrin-dependent and fast endophilin mediated endocytosis represent mechanisms of receptor-mediated endocytosis. In both cases, cargo/ligand binding to the receptor leads to the assembly of adaptor and coat proteins around the forming

endosome which promote receptor and cargo internalisation (Boucrot et al., 2015; Casamento and Boucrot, 2020; Haucke, 2006; Traub and Bonifacino, 2013). In contrast, macropinocytosis is a calcium-dependent endocytic pathway where cargo is internalised *via* membrane remodelling events as opposed to receptor-mediated initiation of endocytosis. Macropinocytosis requires extracellular calcium to initiate an intracellular signalling cascade which stimulates characteristic actin remodelling required for engulfment of cargoes (Canton et al., 2016). To date a requirement for extracellular calcium has not been documented for other forms of endocytosis in non-neuronal cell types (Casamento and Boucrot, 2020; Kumari and Mayor, 2008; Lundmark et al., 2008; Sathe et al., 2018). Macropinocytosis is not defined by specific protein or cellular markers, although large dextran polymers (70 kDa and above) have been shown to be *bona fide* macropinocytosis cargo and thus often used as a marker of the process (Li et al., 2015).

We determined that macropinocytosis was a key endocytic pathway regulating Lp(a) uptake in liver cells, likely through the apo(a) protein component. Consistent with this, we found EGTA effectively inhibited Lp(a) uptake in liver cells and macrophages. Amiloride and its derivative EIPA (5-(N-ethyl-N-isopropyl)-Amiloride) effectively inhibit macropinocytosis by lowering the pH directly below the membrane, preventing activation of the GTPases Rac1 and CDC42, which are required for actin remodelling (Koivusalo et al., 2010). Accordingly, we found that these inhibitors significantly diminished Lp(a) uptake in liver cells and macrophages. These initial results were notable for two key reasons: they identified macropinocytosis as a key endocytic mechanism involved in Lp(a) uptake and it highlighted the importance of the apo(a) component in uptake.

The tricyclic antidepressant imipramine is another newly identified macropinocytosis inhibitor (Lin et al., 2018). Using this drug to validate our data, we found that Lp(a) uptake was partially inhibited in THP-1 macrophages in the presence of imipramine. In contrast, imipramine significantly *stimulated* Lp(a) uptake in liver cells, leading us to determine the effect of the more commonly used selective serotonin reuptake inhibitors (SSRIs) antidepressants had on Lp(a) uptake. We found that citalopram also robustly stimulated Lp(a) uptake into liver cells, while inhibiting uptake into macrophages. Conversely, sertraline inhibited uptake into both cell types, while fluoxetine inhibited uptake only in macrophages.

Finally, we sought to define how imipramine and citalopram regulate Lp(a) uptake and whether this influenced Lp(a) macropinocytosis. Neither drug enhanced macropinocytosis, but rather stimulated Lp(a) binding to the cell surface. Following uptake, imipramine and citalopram stimulated delivery of Lp(a) to Rab11-positive recycling endosomes, and increased recycling of apo(a) into the cellular media. Together, these findings firmly establish macropinocytosis as a key endocytic mechanism responsible for Lp(a) uptake and reveals that antidepressants are important regulators of Lp(a) binding.

Results

Lp(a) uptake is mediated by macropinocytosis.

To first establish if Lp(a) uptake occurs via macropinocytosis, we investigated the requirement of extracellular calcium for Lp(a) uptake into HepG2 liver cells. Extracellular calcium was depleted from the cellular media using 2.5 mM EGTA for 1 hour prior to Lp(a) addition. Lp(a) was added to HepG2 cells for 1 hour following which cells were fixed, permeabilised and Lp(a) detected. To quantify Lp(a) endocytosis, cells were imaged by confocal microscopy using identical settings within the independent experiment and image threshold applied to remove Lp(a) signal at the plasma membrane to allow specific identification of endosomal Lp(a) vesicles (Figure S1). Image quantification confirmed that Lp(a) uptake strictly requires the presence of extracellular calcium, with EGTA almost completely abolishing Lp(a) uptake (Figure 1A,B).

To confirm that macropinocytosis was responsible for Lp(a) uptake, we utilised the widely used macropinocytosis inhibitor, the amiloride analogue 5-(N-Ethyl-N-isopropyl)amiloride (EIPA) (Koivusalo et al., 2010). While EIPA predominantly inhibits macropinocytosis, it is also capable of inhibiting fast endophilin mediated endocytosis (Boucrot et al., 2015). Fast endophilin mediated endocytosis strictly requires growth factors present in serum (Boucrot et al., 2015; Casamento and Boucrot, 2020) therefore to minimise any potential contribution of this alternate endocytic pathway, all experiments were performed in serum free media following a minimum of 1 hour serum starvation. Specific inhibition of macropinocytosis by addition of EIPA in serum free media lead to robust inhibition of Lp(a) uptake (Figure 1C,D) confirming macropinocytosis is an important endocytic mechanism for Lp(a) internalisation.

Macropinocytosis also represents an important endocytic uptake mechanism for native LDL in macrophages during atherogenesis (Kruth, 2011; Kruth et al., 2005). While native LDL uptake by macropinocytosis in the liver or HepG2 cells has not been documented, we sought to exclude a contribution of the LDL moiety of Lp(a) in Lp(a) macropinocytosis by specifically investigating the apo(a) protein component. HEK923 cells were transfected with an apo(a)-cDNA construct fused to the fluorescent protein, mScarlet. Cell media was collected 4 days post transfection, cell debris pelleted and apo(a)-mScarlet concentrated by centrifugation of the media in a 100 kDa molecular weight cut off spin column. The concentrated apo(a)-mScarlet did not contain any apoB (Fig S2A) and was capable of forming Lp(a) when incubated with plasma from a human apoB expressing mouse (Fig S2B). Concentrated apo(a)-mScarlet is therefore an appropriate system for probing the function of apo(a) alone. Inhibition of macropinocytosis with EIPA in serum free media also inhibited apo(a)-mScarlet uptake (Figure 1E,F). Lp(a) macropinocytosis is therefore likely mediated by the apo(a) component of Lp(a).

We next sought to confirm that Lp(a) uptake by macropinocytosis was not specific to HepG2 cells, but rather represents a broad endocytic mechanism to internalise Lp(a). We differentiated THP-1 monocytes into macrophages using PMA. Both EGTA (Figure 2A,B) and amiloride (Figure 2C,D) inhibited Lp(a) uptake, consistent with our results in HepG2 cells and supporting Lp(a) uptake being regulated by macropinocytosis. To provide additional confirmation that Lp(a) uptake is regulated by macropinocytosis we used the tricyclic antidepressant imipramine. Imipramine has been recently identified as an inhibitor of the macropinocytic process in macrophages, and crucially does not inhibit other common endocytic entry routes into the cell (Lin et al., 2018). Imipramine inhibited Lp(a) uptake in macrophages to a level similar to amiloride (Figure 2E, G). Further, imipramine inhibited Lp(a) and 70 kDa dextran uptake (Figure 2E-H), providing further confirmation that macropinocytosis is responsible for Lp(a) uptake.

Antidepressants are modulators of Lp(a) uptake.

Antidepressants have been long observed to increase circulating HDL and LDL levels (Fjukstad et al., 2016; McIntyre et al., 2006; Pan et al., 2018; Rami et al., 2018; Wei et al., 2009). As the antidepressant imipramine inhibited Lp(a) uptake in THP-1 macrophages, we queried whether clinically used SSRI antidepressants were capable of modulating Lp(a) uptake into THP-1. The SSRIs citalopram, fluoxetine and sertraline all inhibited Lp(a) and dextran uptake into differentiated THP-1 macrophages following overnight treatment (Fig2G-H), indicating SSRIs reduce Lp(a) uptake into macrophages by inhibiting macropinocytosis.

We next evaluated the effects of antidepressants in HepG2 cells. Unexpectedly, imipramine treatment stimulated Lp(a) uptake in HepG2 cells in a concentration-dependent manner (Figure 3A,B). Treatment of HepG2 cells with 20 µM imipramine overnight lead to an average ~280% increase in Lp(a) uptake into the cell across seven independent experiments (Figure 3C), strongly indicating that imipramine is a robust stimulator of Lp(a) uptake into liver cells.

Similar to imipramine, overnight treatment with the SSRI citalopram induced robust, concentration-dependent increases in Lp(a) uptake (Figure 3D-F). The SSRIs fluoxetine and sertraline were applied for 2 hours prior to Lp(a) uptake as overnight treatments were not well tolerated in HepG2 cells. Fluoxetine did not alter Lp(a) uptake (Figure 3G-I). In contrast, sertraline induced a concentration-dependent inhibition of Lp(a) uptake (Figure 3J-L). Unexpectedly, dextran uptake was not increased with imipramine or citalopram treatment and was inhibited by fluoxetine and sertraline treatments (Figure 3M,N). Imipramine and citalopram therefore do not stimulate Lp(a) uptake by inducing macropinocytosis in liver cells. Together these results demonstrate that SSRIs are clinically important modulators of Lp(a) uptake with differential effects between liver and macrophage cell types.

Imipramine and citalopram stimulate Lp(a) binding to the cell surface.

We next sought to understand how imipramine and citalopram stimulated Lp(a) uptake in liver cells. We hypothesised that imipramine or citalopram may be stimulating Lp(a) uptake by increasing Lp(a) binding to the plasma membrane, which could then allow higher levels of engulfment without directly stimulating macropinocytic processes. To test this, we performed experiments specifically investigating Lp(a) and dextran bound to the cell surface. HepG2 cells were treated with imipramine or citalopram overnight, cooled to prevent endocytic uptake occurring and the amount of Lp(a) or dextran-TRITC bound quantified. Lp(a) was detected by incubation of the LPA4 antibody and corresponding secondary antibody to chilled cells, while dextran was detected directly. Consistent with imipramine and citalopram stimulating Lp(a) surface binding, Lp(a) levels on the cell surface were increased following treatment in HepG2 cells (Figure 4A,B). Conversely, dextran surface binding was unaltered by imipramine and citalopram treatment (Figure 4C,D), confirming that the increase in Lp(a) macropinocytosis induced by imipramine and citalopram is due to specific, enhanced Lp(a) binding to the plasma membrane.

To further confirm the effect of citalopram on HepG2 cells, cells were citalopram treated overnight, glutaraldehyde-fixed and imaged using scanning electron microscopy. Citalopram treatment lead to formation of distinct protrusions projecting from the plasma membrane (Figure 4E,F, white arrows). These plasma membrane alterations are consistent with the increased microvilli observed in HepG2 cells that facilitate immune cell adhesion to the plasma membrane (Reglero-Real et al., 2014). Citalopram is therefore potentially increasing the adhesion of Lp(a) and apo(a) to the plasma membrane by inducing formation of actin-rich microvilli.

Antidepressants stimulate Lp(a) and apo(a) recycling.

Previously, we determined that following internalisation, the apo(a) protein component of Lp(a) is specifically recycled back into the extracellular environment while the LDL component was targeted to the lysosome (Sharma et al., 2017). We therefore tested the effect imipramine and citalopram exerted on the endosomal sorting of Lp(a) and apo(a) into recycling compartments of the cell.

Lp(a) was added to HepG2 cells for 30 or 120 minutes following overnight imipramine/citalopram treatment, cells fixed, permeabilised and co-stained for Lp(a) and Rab11 (recycling endosomes), Rab7 (late endosomes) or LAMP1 (lysosomes). Cells were then imaged by confocal microscopy and co-localisation between Lp(a) and endosomal compartment markers determined by overlap of threshold-defined endosomal signals between channels to exclude contribution of plasma membrane signal.

After 30 minutes of incubation, Lp(a) co-localisation with Rab11 was significantly increased with imipramine and citalopram treatments compared to vehicle control (Figure 5A, E). No significant difference in Lp(a) and Rab11 co-localisation was observed between vehicle control and imipramine/citalopram following 120 minutes of Lp(a) incubation (Figure 5B,E). No significant difference between vehicle control and imipramine/citalopram treated cells was observed in Lp(a) co-localisation with either Rab7 (Figure 5C,D,F) or LAMP1 (Figure S3 A-C) at any timepoint. Apo(a) co-localisation with Rab11 was significantly increased by citalopram treatment compared to vehicle at both the 30 and 120-minute timepoints, while imipramine did not induce any significant changes to apo(a) colocalisation (Figure S4A-C). These results are concordant with our previous study showing Lp(a) is sorted primary to recycling and not degradative compartments within the cell (Sharma et al., 2017) and indicates imipramine and citalopram specifically induce delivery of Lp(a) into Rab11^{+} recycling endosomes.

We next tested the functional impact of the antidepressant-induced alterations to Lp(a) and apo(a) recycling by Western blot. Lp(a) or apo(a) were added to vehicle, imipramine or citalopram treated HepG2 cells for 2 hours in serum free media. Lp(a)/apo(a) containing media was then removed, cells washed, and fresh media added. This media was then immediately collected, and cells lysed for baseline uptake and recycling measurements, or incubated in the fresh media for 2 or 6 hours to assess Lp(a)/apo(a) retention within the cell and recycling to the media.

Both imipramine and citalopram treatment significantly increased the Lp(a) signal within the cell across all time points compared to the vehicle control (Figure 6A,B). Imipramine and citalopram treatments also significantly increased Lp(a) recycling into the cellular media over time compared to the vehicle control (Figure 6C,D), consistent with the observed increase in co-localisation with Rab11 induced by these antidepressants (Figure 5A,E).

Citalopram treatment significantly increased apo(a) signal within the cell across all time points compared to the vehicle control, while imipramine treatment lead to an increase in apo(a) signal approaching statistical significance ($p=0.0515$) (Figure 6D,E). In contrast to Lp(a), citalopram treatment alone leads to a significant increase in apo(a) recycling to the cellular media (Figure 6I,J), consistent with the citalopram-specific increase in apo(a) colocalisation with Rab11 observed (Figure S4). Together, these results indicate that imipramine and citalopram increase Lp(a) and apo(a) uptake into the cell, increase their delivery to cellular recycling compartments and subsequent stimulate recycling into the cellular media.

Discussion

Endocytosis is the central regulator of lipoprotein clearance from circulation (Zanoni et al., 2018). The uptake of LDL via the LDLR is the most well characterised of the lipoprotein endocytosis pathways (Goldstein and Brown, 2009, 1974). In contrast, the endocytic mechanisms mediating the uptake of the LDL-like, Lp(a) molecule are not well understood (McCormick and Schneider, 2019; Zanoni et al., 2018). In this study we have established that Lp(a) uptake occurs via the fluid-phase endocytic mechanism macropinocytosis (Fig 7). In defining this process, we have found that Lp(a) uptake is: (1) mediated by the apo(a) protein component, (2) dependent on extracellular calcium, (3) inhibited by amiloride/EIPA, and (4) occurs in a manner analogous to the canonical marker of macropinocytosis, 70 kDa dextran in liver cells and macrophages. In our efforts to pharmacologically define the macropinocytic uptake of Lp(a), we discovered that common antidepressants exert complex effects on Lp(a) uptake (Fig 7). The tricyclic antidepressant, imipramine and the SSRIs, citalopram, sertraline and fluoxetine all inhibit Lp(a) uptake by macropinocytosis in THP-1 macrophages. In HepG2 liver cells, imipramine and citalopram stimulated Lp(a) uptake by increasing Lp(a) binding to the cell surface rather than increasing the rate of macropinocytosis *per se*. Antidepressant stimulated Lp(a) uptake resulted in functional consequences, with imipramine and citalopram treatment resulting in increased Lp(a) delivery into recycling, but not degradative compartments, resulting in increased recycling of Lp(a)-derived apo(a) into the cellular media.

Uptake by macropinocytosis represents a new paradigm for Lp(a) clearance from circulation. Other modes of endocytosis such as clathrin-dependent endocytosis or fast endophilin mediated endocytosis occur following ligand: receptor binding (Casamento and Boucrot, 2020; Redpath et al., 2020). In contrast, macropinocytosis occurs following extensive membrane remodelling to form a macropinocytic cup in which cargoes are engulfed (Kerr and Teasdale, 2009). Imipramine and citalopram enhanced binding of Lp(a) to the plasma membrane suggests that membrane anchoring provides a further layer of regulation upon Lp(a) uptake. The apo(a) homologue, plasminogen has been shown to bind to cell surface actin (Miles et al., 2006), following which endocytosis occurs (Briens et al., 2017). Similar to plasminogen, Lp(a) has been previously described to bind to the cell surface via interaction with actin (Dudani and Ganz, 1996). Furthermore, Lp(a) has been shown to stimulate actin remodelling in endothelial cells (Pellegrino et al., 2004).

Entry of Lp(a) into the cell via macropinocytosis aligns well with the lack of any clear receptor-mediated process being reported for Lp(a) uptake. At least twelve receptors have been proposed to mediate Lp(a) uptake into the cell, yet no receptor has been shown to play a definitive role in mediating this uptake (McCormick and Schneider, 2019). Lp(a) binds to receptors such as the plasminogen receptor $PlgR_{KT}$ and SR-BI (Sharma et al., 2017; Yang et al., 2013) which have been demonstrated to bind other ligands (plasminogen, HDL respectively) to the plasma membrane while not inducing receptor-mediated endocytosis (Marques et al., 2019; Miles et al., 2012). We propose that for at least a subset of the receptors implicated in Lp(a) uptake, these receptors act not as mediators of Lp(a) internalisation into the cell, but rather as membrane anchors immobilising Lp(a) to the plasma membrane and allowing macropinocytic engulfment to occur.

Links between depression and increased atherosclerotic cardiovascular disease development have been long observed (Chávez-Castillo et al., 2018; Hare et al., 2014). Exacerbating the increased atherosclerosis risk in depression is the well-established relationship between antidepressant use and increased circulating levels of the atherogenic LDL (McIntyre et al., 2006; Pan et al., 2018; Wei et al., 2009). In contrast, links between depression, Lp(a) and antidepressant use have been rarely studied. Circulating Lp(a) levels have been observed to be increased in patients with severe depression

(Emanuele et al., 2006; Hamidifard et al., 2009), while a double-blinded interventional study showed that treatment with the SSRI paroxetine but not the tricyclic antidepressant amitriptyline decreased circulating Lp(a) levels (Paslakis et al., 2011). Our *in vitro* data clearly support the *in vivo* link between Lp(a) metabolism and antidepressants and provide a mechanistic basis as to how specific antidepressants may reduce Lp(a) levels in circulation by increasing Lp(a) macropinocytosis. These results have important implications regarding the use of SSRIs in patients with high Lp(a): citalopram may potentially reduce Lp(a) levels in circulation by boosting uptake, while sertraline may increase circulating levels by inhibiting uptake.

Our data show that imipramine and citalopram increase Lp(a) uptake into liver cells where Lp(a) catabolism is primarily proposed to occur (Cain et al., 2005). Furthermore, both drugs promote apo(a) recycling after Lp(a) uptake. The function of apo(a) recycling following Lp(a) uptake is still unclear. We have previously found that following internalisation into liver cells, the apo(a) protein component is removed from the LDL-like component of Lp(a), and rather than undergoing lysosomal or proteasomal degradation is re-secreted to the extracellular space (Sharma et al., 2017). Free apo(a) has been long identified in circulation and urine in consistently proteolysed forms in both healthy patients (Edelstein et al., 1999; Mooser et al., 1996) and nephrotic syndrome patients (Doucet et al., 2000) that is consistent with extracellular metalomatrix protease degradation of free apo(a) in the extracellular environment *in vitro* and in mouse plasma *in vivo* (Edelstein et al., 1997, 1999). Together, these studies indicate that when apo(a) is free in the extracellular environment it may be susceptible to cleavage by extracellular proteases and then removed from the body in the urine. We hypothesise that recycling serves as a mechanism to remove the LDL-like component of Lp(a), releasing free apo(a) into circulation for proteolysis and excretion from the body. Our finding that imipramine and citalopram stimulate apo(a) recycling indicates these drugs may lead to increased apo(a) degradation and decreased circulating Lp(a) levels *in vivo*.

An interesting implication of our study is the potential use of commonly used antidepressants as nuanced manipulators of endocytic processes. Imipramine was recently identified as an inhibitor of macropinocytosis (Lin et al., 2018) , yet our data suggests this inhibition is cell-type dependent. In macrophages, which can undertake constitutive and stimulated macropinocytosis (Canton et al., 2016), imipramine and citalopram were robust macropinocytosis inhibitors. In HepG2 liver cells, imipramine and citalopram had no effect on dextran macropinocytosis, yet was capable of increasing Lp(a) macropinocytosis by increasing binding to the plasma membrane. Citalopram also stimulates endocytosis of its main target, the serotonin transporter, and cholera toxin in serotonergic neurons (Lau et al., 2008) indicting citalopram is capable of stimulating the uptake of multiple protein cargoes in diverse cell types, while also acting as a macropinocytosis inhibitor in macrophages. Sertraline and fluoxetine inhibited macropinocytosis in both liver and macrophage cell types. Sertraline and fluoxetine are also established dynamin inhibitors, in contrast to imipramine and citalopram (Otomo et al., 2008). Macropinocytosis is a dynamin-independent process (Cao et al., 2007; Li et al., 2015), indicating that perhaps fluoxetine and sertraline inhibit macropinocytosis by interfering with other regulators of macropinocytosis. Altogether, our data and others indicate antidepressants have complex effects on endocytic processes that are cargo and cell-type dependant.

Questions remain from our current study that need to be addressed to better understand the effects of antidepressants on Lp(a) uptake. This study was entirely *in vitro* in nature, confirmation of the effects of the antidepressants on Lp(a) macropinocytosis need to be verified in mouse models and clinical trials of depression sufferers to confirm their effects *in vivo*. While we have identified that surface binding appears to be an important mediator of Lp(a) uptake, we have not yet identified

specific mediators of this surface binding. Future studies evaluating the plasma membrane binding of Lp(a) in cells depleted of receptors implicated in Lp(a) uptake will prove informative as to how this surface binding is regulated. Further, the cause of the disparity of the effects of antidepressants between liver cells and macrophages remains unknown. Discovering why antidepressants have differing effects on macropinocytosis between cell types would be of interest for both a fundamental understanding of endocytic processes and for understanding the systemic effects of these drugs.

In conclusion, our data suggest that macropinocytosis regulates Lp(a) uptake, indicating that modulation of macropinocytic uptake may be a potential therapeutic avenue for reducing Lp(a) levels. As modulators of macropinocytosis, our study strongly indicates that antidepressants, especially the SSRI citalopram, should be investigated pre-clinically and clinically for their effects on Lp(a) levels in circulation. The benefit of identifying SSRIs that are capable of reducing Lp(a) levels *in vivo* are clear. Depression sufferers are less likely to adhere to treatments for co-morbidities such as cardiovascular disease (Gehi et al., 2005; Goldstein et al., 2017; Grenard et al., 2011). SSRIs that reduce Lp(a) levels in depression sufferers would allow treatment of their mental health and Lp(a)-induced atherosclerotic burden with a single medicine, improving their quality of life and cardiovascular health with the maximum likelihood of compliance.

Acknowledgements

This research was supported by project grants from the Royal Society of New Zealand (Marsden Fund 17-UOO-081) and the Health Research Council of New Zealand (18/207).

Author contributions

GMIR, ND, HS, GM and NK performed the experiments. MR and MW obtained and purified the Lp(a). GMIR, ND and NA analysed the data. GMIR, ND and SPAM prepared the figures and wrote the manuscript. ND prepared the schematic. GR, ND and SPAM supervised the students. GR and SPAM conceived of the study.

Declaration of Interests

All authors declare no competing interests.

Methods

Key Resources Table

REAGENT or RESOURCE	SOURCE	IDENTIFIER
Antibodies		
Rabbit anti-LAMP1	Cell Signaling Technology	Cat# 9091; RRID: AB_2687579
Anti-Apolipoprotein(a) antibody, clone LPA4	Millipore	Cat#MABS1284
Goat polyclonal anti-Lp(a) antibody	Wako Pure Chemical Industries (Osaka, Japan)	Cat#
Rabbit monoclonal anti-Rab7 [EPR7589]	Abcam	Cat#ab137029; RRID: AB_2629474
Rabbit anti-Rab11	Cell Signaling Technology	Cat# 5589; RRID: AB_10693925
Rabbit monoclonal anti-Lp(a) antibody	Abcam	Cat# ab208184
Mouse monoclonal anti-apoB antibody clone 1D1		
Donkey anti-Mouse IgG (H+L) Highly Cross-Adsorbed Secondary Antibody, Alexa Fluor 488	Thermo Fisher Scientific	Cat# A-21202, RRID:AB_141607
Donkey anti-Mouse IgG (H+L) Highly Cross-Adsorbed Secondary Antibody, Alexa Fluor 594	Thermo Fisher Scientific	Cat# A-21203, RRID:AB_141633
Donkey anti-Rabbit IgG (H+L) Highly Cross-Adsorbed Secondary Antibody, Alexa Fluor 488	Thermo Fisher Scientific	Cat# A-21206, RRID:AB_2535792
Donkey anti-Rabbit IgG (H+L) Highly Cross-Adsorbed Secondary Antibody, Alexa Fluor 594	Thermo Fisher Scientific	Cat# A-21207, RRID:AB_141637
Biological Samples		
Purified human Lp(a)		
Chemicals, Peptides, and Recombinant Proteins		
Phosphate buffered saline, pH 7.4	Gibco	Cat#10010023
DMEM, high glucose	Gibco	Cat#11965092
RPMI 1640 medium	Gibco	Cat#11875119
Fetal Bovine Serum, qualified, New Zealand	Gibco	Cat#10091155
Penicillin-Streptomycin (10,000 U/mL)	Gibco	Cat#15140122

Amphotericin B	Gibco	Cat#15290018
TrypLE™ Express Enzyme (1X), no phenol red	Gibco	Cat#12604021
Dextran, Tetramethylrhodamine, 70,000 MW, Lysine Fixable	Invitrogen	Cat#D1818
Dextran, Oregon Green 488; 70,000 MW, Anionic, Lysine Fixable	Invitrogen	Cat#D7173
5-(N-Ethyl-N-isopropyl)amiloride	Sigma-Aldrich	Cat#A3085
Amiloride hydrochloride hydrate	Sigma-Aldrich	Cat#A7410
Ethylene glycol-bis(2-aminoethylether)-N,N,N′,N′-tetraacetic acid	Sigma-Aldrich	Cat#E3889
ProLong™ antifade mounting reagent	Invitrogen	Cat#P36934
Triton-X100	Bio-Rad Laboratories	Cat#1610407
Tween-20	Bio-Rad Laboratories	Cat#1706531
TEMED	Bio-Rad Laboratories	Cat#1610801
Precision Plus Protein™ All Blue Prestained Protein Standards	Bio-Rad Laboratories	Cat#1610373
Bolt™ 4 to 12%, Bis-Tris, 1.0 mm, Mini Protein Gel, 10-well	Invitrogen	Cat#NW04120BOX
Imipramine hydrochloride	Sigma-Aldrich	Cat#I7379
Sertraline tablets 50 mg as hydrochloride	Teva Pharmaceutical Industries Limited	
Fluoxetine tablets 20 mg as hydrochloride	Teva Pharmaceutical Industries Limited	
Citalopram tablets 20 mg as hydrobromide	PSM Healthcare Limited	
Phorbol 12-myristate 13-acetate	Sigma-Aldrich	Cat#P1585
Paraformaldehyde	Sigma-Aldrich	Cat#P6148
Goat Serum, New Zealand origin	Sigma-Aldrich	Cat#16210064
Plasminogen from human plasma	Athens Research and Technology	Cat#16-16-161200
Alexa Fluor 488 Microscale Protein labelling kit	Life Technologies	Cat#A30006
Qubit Protein Assay Kit	Thermo Fisher Scientific	Cat#Q33211
Pierce Protein Concentrator PES, 100K MWCO, 5-20 mL	Thermo Fisher Scientific	Cat#88532
Lipofectamine 3000	Life Technologies	Cat#L3000015
Deposited Data		
Figshare		
Experimental Models: Cell Lines		
HepG2	ATCC	ATCC Cat# HB-8065, RRID:CVCL_0027
THP-1	ATCC	ATCC Cat# TIB-202, RRID:CVCL_0006
HEK293	ATCC	ATCC Cat# CRL-1573, RRID:CVCL_0045
Recombinant DNA		
Lipoprotein a (LPA) (NM_005577) Human Tagged ORF Clone	Origene	CAT#RG212070
Software and Algorithms		
Prism	Graphpad	RRID:SCR_002798
FIJI		RRID:SCR_002285
Fluoview FV-10 ASW	Olympus	RRID:SCR_014215

Resource Availability

Lead contact

Further information and requests for resources and reagents should be directed to and will be fulfilled by the Lead Contact, Professor Sally PA McCormick (sally.mccormick@otago.ac.nz).

Data and Code Availability

The raw confocal imaging data has been deposited into the FigShare repository doi:
FIJI Macros are available upon request.

Experimental Model and Subject Details

Cell culture

Cells were grown at 37°C in a 5% CO_2 humidified incubator. HepG2 cells (ATCC, CVCL-2205) and HEK293 cells (ATCC, CVCL_0045) were cultured in DMEM with 10% FBS, 100 u/ml penicillin, 100µg/ml streptomycin, and 0.25 µg/mL amphotericin B. THP-I cells (ATCC, CVCL_0006) were cultured in RPMI with 10% FBS, 100 u/ml penicillin, 100µg/ml streptomycin, and 0.25 µg/mL amphotericin B. THP-I cells were differentiated for 72 hours prior to use with 100 nM Phorbol 12-myristate 13-acetate (PMA) (Sigma-Aldrich).

Lp(a) enrichment from patient samples

Lp(a) was isolated from plasma samples from healthy individuals from the Otago LPA cohort (Morgan et al., 2020) with Lp(a) levels >50 mg/dL (equivalent to 108 nmol/L using a conversion factor of 2.15). Individual samples used for isolation had apo(a) isoform sizes ranging from 17-20 with a predominant apo(a) isoform size of 19. 100 µg (HepG2) or 200 µg (THP-I) by total protein concentration of enriched Lp(a) was used per well. Purified Lp(a) protein levels were quantified using the Qubit Protein Assay Kit (Thermo Fisher Scientific).

Ethical Approval

Ethical approval for the samples used in this study was granted by the Lower Regional South Ethics Committee (LRS/12/01/005).

Method Details

Drug treatments

For imipramine and citalopram treatments, cells were treated overnight prior to the experiment. Two hours before addition of Lp(a)/apo(a), cells were transferred into serum-free media and new imipramine/citalopram added. For sertraline and fluoxetine treatments in HepG2 cells, cells were transferred into serum-free media two hours prior to Lp(a)/apo(a) addition. For sertraline and fluoxetine treatments in THP-I cells, cells were treated overnight prior to the experiment. Two hours before addition of Lp(a)/apo(a), cells were transferred into serum-free media and new sertraline/fluoxetine added. For amiloride/EIPA/EGTA treatments, cells were transferred into serum-free media one hour prior to Lp(a)/apo(a) addition.

Immunofluorescence staining

Cells were fixed with 4% paraformaldehyde for 15 minutes at 37ºC in a humidified incubator. Cells were then washed with PBS and blocked with 3% goat serum. The antibodies used in this study were: The secondary antibodies include goat anti-rabbit Alexa Fluor 594, anti-mouse Alexa Fluor 488, and

anti-rabbit Alexa Fluor 594 (ThermoFisher Scientific, 1:1000). Slides were mounted with ProLong™ antifade mounting medium (Invitrogen).

Confocal imaging

All coverslips were imaged on an Olympus FV1000/1200/3000 confocal microscope using 405, 488 and 561 nm laser lines with a 60x, NA 1.4 oil immersion lens. Within each experiment, images from each coverslip were captured using identical laser power, gain, offset and PMT (FV1000/1200)/GaAsP(FV3000) detector voltage. The maximum field of view was captured at a pixel size of ~125-135 nm.

Electron microscopy

All the steps were carried out in a PELCO Biowave microwave processor (TedPellaInc., Redding, CA, USA). PFA fixed samples on coverslips were first re- fixed in 2.5% glutaraldehyde in 0.1 M sodium cacodylate buffer, washed with 0.1 M sodium cacodylate buffer followed by post-fixation with 1% OsO4 (osmium tetroxide) (ProScitech) in cacodylate buffer. Following buffer and water washes, fixed samples were serially dehydrated in increasing percentages of ethanol and finally dried in a critical point drier. Dried samples were mounted on stubs, sputter coated with platinum and imaged using a FEI Nova NanoSEM 230 at 5 kV.

Immunoblotting

After denaturing in sodium dodecyl sulfate (SDS), samples were subjected to 10% SDS–polyacrylamide gel electrophoresis and transferred to nitrocellulose transfer membranes. Cultured cells were washed twice with ice cold PBS and lysed in radioimmune precipitation assay (RIPA) buffer containing 20 mm Tris HCl, pH 7.5, 150 mm NaCl, 1 mm EDTA, 1 mm EGTA, 1% Triton X-100, 2.5 mm sodium pyrophosphate, 1 mm β-glycerophosphate, 1 mm Na3VO4, 1 mm NaF, and 1× protease inhibitor mixture (Roche Applied Science). After incubation on ice for 10 min, cell lysates were subjected to centrifugation at 15,000 rpm for 10 min. 60 μg of total lysates were subjected to 4-12% sodium dodecyl sulfate polyacrylamide gradient gel electrophoresis and transferred onto membranes. Membranes were blocked in 5% skim milk buffer in PBS with 0.1% Triton-X for 1 h and incubated with primary antibodies at 4°C overnight followed by probing with fluorescence labelled secondary antibodies. Proteins were detected with the Odyssey Infrared Imaging System (LI-COR Biosciences). Densitometry was analysed with FIJI/ImageJ software.

Apo(a) expression and concentration

Apo(a)-mScarlet was transfected into HEK293 cells using Lipofectamine 3000. 4 days post transfection, cell media was collected, cooled and centrifuged at 3000g to pellet cellular debris. Media was then transferred into a 20 mL, 100 kDa MW cutoff centrifuge tube (Thermo Fisher Scientific) and centrifuged at 3000g at 4°C until media volume was 5x concentrated. Concentrated media was frozen until used.

Immunoprecipitation of cell media for recycling experiments

To detect the secretion of Lp(a) particles into culture media following incubation with the purified lipoprotein, culture media was collected and immunoprecipitated prior to analysis by western blot. Following 2h incubation with Lp(a) in a humidified 37°C incubator to foster maximal uptake of the lipoprotein, culture media was removed, cells washed 5x with PBS, and fresh media added to cells. Media was harvested from 0-6h post-treatment and incubated with a solution of polyclonal Lp(a) antibody (WAKO) immobilised on Protein G magnetic beads (Thermo Fisher Scientific). Lp(a) was

immunoprecipitated from the media overnight at 4°C and eluted under reducing conditions. Samples were then subjected to western blotting using LPA4 antibody.

Ethical Approval

Ethical approvals for patient samples used in this study were granted by the Lower Regional South Ethics Committee (LRS/12/01/005).

Quantification and Statistical Analysis

Image Quantification

Images were quantified using FIJI (Schindelin et al., 2012). Custom macros were created for endosome identification and overlap analysis. For endosome identification, a single intensity-based threshold per experiment was used to identify Lp(a)/apo(a) endosomes and nuclei. For overlap analysis, one intensity-based threshold was used to identify Lp(a)/apo(a) endosomes, and another used to identify Rab7/11/LAMP1 compartments. The same threshold was used for each image in a single experiment. The threshold was used to generate a mask for each channel, and the Lp(a)/apo(a) mask subtracted from the inverted Rab7/11/LAMP1 mask to generate an overlap mask of Lp(a)/apo(a) present in the Rab7/11/LAMP1 compartment. The number of Lp(a)/apo(a) endosomes in the overlap mask was quantified and divided by the total number of Lp(a)/apo(a) endosomes to determine the percentage of total Lp(a)/apo(a) endosomes overlapping with Rab7/11/LAMP1 compartments.

Data Representation and Statistical analysis

Data are expressed as means of independent experiments +/- SEM. Statistical analyses were performed with Prism Software version 8 (GraphPad Software).

References

Argraves, K.M.T., Kozarsky, K.F., Fallon, J.T., Harpel, P.C., and Strickland, D.K. (1997). The atherogenic lipoprotein Lp(a) is internalized and degraded in a process mediated by the VLDL receptor. J. Clin. Invest. *100*, 2170–2181.

Boerwinkle, E., Leffert, C.C., Lin, J., Lackner, C., Chiesa, G., and Hobbs, H.H. (1992). Apolipoprotein(a) gene accounts for greater than 90% of the variation in plasma lipoprotein(a) concentrations. J. Clin. Invest. *90*, 52–60.

Boucrot, E., Ferreira, A.P.A., Almeida-Souza, L., Debard, S., Vallis, Y., Howard, G., Bertot, L., Sauvonnet, N., and McMahon, H.T. (2015). Endophilin marks and controls a clathrin-independent endocytic pathway. Nature *517*, 460–465.

Briens, A., Bardou, I., Lebas, H., Miles, L.A., Parmer, R.J., Vivien, D., and Docagne, F. (2017). Astrocytes regulate the balance between plasminogen activation and plasmin clearance via cell-surface actin. Cell Discov. *3*, 1–18.

Cain, W.J., Millar, J.S., Himebauch, A.S., Tietge, U.J.F., Maugeais, C., Usher, D., and Rader, D.J. (2005). Lipoprotein [a] is cleared from the plasma primarily by the liver in a process mediated by apolipoprotein [a]. J. Lipid Res. *46*, 2681–2691.

Canton, J., Schlam, D., Breuer, C., Gütschow, M., Glogauer, M., and Grinstein, S. (2016). Calcium-sensing receptors signal constitutive macropinocytosis and facilitate the uptake of NOD2 ligands in macrophages. Nat. Commun. *7*, 11284.

Cao, H., Chen, J., Awoniyi, M., Henley, J.R., and McNiven, M.A. (2007). Dynamin 2 mediates fluid-phase micropinocytosis in epithelial cells. J. Cell Sci. *120*, 4167–4177.

Casamento, A., and Boucrot, E. (2020). Molecular mechanism of Fast Endophilin-Mediated Endocytosis. Biochem. J. *477*, 2327–2345.

Chaudhary, R., Garg, J., Shah, N., and Sumner, A. (2017). PCSK9 inhibitors: A new era of lipid lowering therapy. World J. Cardiol. *9*, 76.

Chávez-Castillo, M., Ortega, Á., Nava, M., Fuenmayor, J., Lameda, V., Velasco, M., Bermúdez, V., and Rojas-Quintero, J. (2018). Metabolic risk in depression and treatment with selective serotonin reuptake inhibitors: are the metabolic syndrome and an increase in cardiovascular risk unavoidable? Vessel Plus *2*, 6.

Chemello, K., Beeské, S., Trang Tran, T.T., Blanchard, V., Villard, E.F., Poirier, B., Le Bail, J.C., Dargazanli, G., Ho-Van-Guimbal, S., Boulay, D., et al. (2020). Lipoprotein(a) Cellular Uptake Ex Vivo and Hepatic Capture In Vivo Is Insensitive to PCSK9 Inhibition With Alirocumab. JACC Basic to Transl. Sci. *5*, 549–557.

Doucet, C., Mooser, V., Gonbert, S., Raymond, F., Chapman, J., Jacobs, C., and Thillet, J. (2000). Lipoprotein(a) in the nephrotic syndrome: Molecular analysis of lipoprotein(a) and apolipoprotein(a) fragments in plasma and urine. J. Am. Soc. Nephrol. *11*, 507–513.

Dudani, A.K., and Ganz, P.R. (1996). Endothelial cell surface actin serves as a binding site for plasminogen, tissue plasminogen activator and lipoprotein(a). Br. J. Haematol. *95*, 168–178.

Edelstein, C., Italia, J.A., and Scanu, A.M. (1997). Polymorphonuclear cells isolated from human peripheral blood cleave lipoprotein(a) and apolipoprotein(a) at multiple interkringle sites via the enzyme elastase. Generation of mini-Lp(a) particles and apo(a) fragments. J. Biol. Chem. *272*, 11079–11087.

Edelstein, C., Shapiro, S.D., Klezovitch, O., and Scanu, A.M. (1999). Macrophage metalloelastase, MMP-12, cleaves human apolipoprotein(a) in the linker region between kringles IV-4 and IV-5: Potential relevance to lipoprotein(a) biology. J. Biol. Chem. *274*, 10019–10023.

Emanuele, E., Carlin, M. V., D'Angelo, A., Peros, E., Barale, F., Geroldi, D., and Politi, P. (2006). Elevated plasma levels of lipoprotein(a) in psychiatric patients: A possible contribution to increased vascular risk. Eur. Psychiatry *21*, 129–133.

Fjukstad, K.K., Engum, A., Lydersen, S., Dieset, I., Steen, N.E., Andreassen, O.A., and Spigset, O. (2016). Metabolic Abnormalities Related to Treatment with Selective Serotonin Reuptake Inhibitors in Patients with Schizophrenia or Bipolar Disorder. J. Clin. Psychopharmacol. *36*, 615–620.

Floren, C., Albers, J.J., and Bierman, E.L. (1981). Pages 636-639 UPTAKE OF Lp (a) LIPOPROTEIN BY CULTURED FIBROBLASTS Abbreviations : Biochem. Biophys. Res. Commun. 636–639.

Gehi, A., Haas, D., Pipkin, S., and Whooley, M.A. (2005). Depression and medication adherence in outpatients with coronary heart disease: Findings from the heart and soul study. Arch. Intern. Med. *165*, 2508–2513.

Goldstein, J.L., and Brown, M.S. (2009). The LDL Receptor. Arterioscler. Thromb. Vasc. Biol. *29*, 431–438.

Goldstein, J.S., and Brown, M.S. (1974). Binding Cultured and Degradation of Low Density Human Fibroblasts Lipoproteins by from. J. Biol. Chem. *249*, 5153–5162.

Goldstein, C.M., Gathright, E.C., and Garcia, S. (2017). Relationship between depression and medication adherence in cardiovascular disease: the perfect challenge for the integrated care team. Patient Prefer. Adherence *Volume 11*, 547–559.

Grenard, J.L., Munjas, B.A., Adams, J.L., Suttorp, M., Maglione, M., McGlynn, E.A., and Gellad, W.F. (2011). Depression and medication adherence in the treatment of chronic diseases in the United States: A meta-analysis. J. Gen. Intern. Med. *26*, 1175–1182.

Hamidifard, S., Fakhari, A., Mahboob, S., and Gargari, B.P. (2009). Plasma levels of lipoprotein (a) in patients with major depressive disorders. Psychiatry Res. *169*, 253–256.

Hare, D.L., Toukhsati, S.R., Johansson, P., and Jaarsma, T. (2014). Depression and cardiovascular disease: A clinical review. Eur. Heart J. *35*, 1365–1372.

Haucke, V. (2006). Cargo Takes Control of Endocytosis. Cell *127*, 35–37.

Hofmann, S.L., Eaton, D.L., Brown, M.S., McConathy, W.J., Goldstein, J.L., and Hammer, R.E. (1990). Overexpression of human low density lipoprotein receptors leads to accelerated catabolism of Lp(a) lipoprotein in transgenic mice. J. Clin. Invest. *85*, 1542–1547.

Kerr, M.C., and Teasdale, R.D. (2009). Defining macropinocytosis. Traffic *10*, 364–371.

Koivusalo, M., Welch, C., Hayashi, H., Scott, C.C., Kim, M., Alexander, T., Touret, N., Hahn, K.M., and Grinstein, S. (2010). Amiloride inhibits macropinocytosis by lowering submembranous pH and preventing Rac1 and Cdc42 signaling. J. Cell Biol. *188*, 547–563.

Kruth, H.S. (2011). Receptor-independent fluid-phase pinocytosis mechanisms for induction of foam cell formation with native low-density lipoprotein particles. Curr. Opin. Lipidol. *22*, 386–393.

Kruth, H.S., Jones, N.L., Huang, W., Zhao, B., Ishii, I., Chang, J., Combs, C.A., Malide, D., and Zhang, W.Y. (2005). Macropinocytosis is the endocytic pathway that mediates macrophage foam cell formation with native low density lipoprotein. J. Biol. Chem. *280*, 2352–2360.

Kumari, S., and Mayor, S. (2008). ARF1 is directly involved in dynamin-independent endocytosis. Nat. Cell Biol. *10*, 30–41.

Langsted, A., and Nordestgaard, B.G. (2020). Lipoprotein(a): Is It More, Less or Equal to LDL as a Causal Factor for Cardiovascular Disease and Mortality? Curr. Opin. Lipidol. *31*, 125–131.

Lau, T., Horschitz, S., Berger, S., Bartsch, D., and Schloss, P. (2008). Antidepressant-induced internalization of the serotonin transporter in serotonergic neurons. FASEB J. *22*, 1702–1714.

Lawn, R.M., Schwartz, K., and Patthy, L. (1997). Convergent evolution of apolipoprotein(a) in primates and hedgehog. Proc. Natl. Acad. Sci. U. S. A. *94*, 11992–11997.

Li, L., Wan, T., Wan, M., Liu, B., Cheng, R., and Zhang, R. (2015). The effect of the size of fluorescent dextran on its endocytic pathway. Cell Biol. Int. *39*, 531–539.

Lin, H.-P.P., Singla, B., Ghoshal, P., Faulkner, J.L., Cherian-Shaw, M., O'Connor, P.M., She, J.-X.X., Belin de Chantemele, E.J., and Csányi, G. (2018). Identification of novel macropinocytosis inhibitors using a rational screen of Food and Drug Administration-approved drugs. Br. J. Pharmacol. *175*, 3640–3655.

Lippi, G., Favaloro, E.J., and Sanchis-Gomar, F. (2020). Antisense lipoprotein[a] therapy: State-of-the-art and future perspectives. Eur. J. Intern. Med. *76*, 8–13.

Liu, Y., Ma, H., Zhu, Q., Zhang, B., Yan, H., Li, H., Meng, J., Lai, W., Li, L., Yu, D., et al. (2019). A genome-wide association study on lipoprotein (a) levels and coronary artery disease severity in a Chinese population. J. Lipid Res. *60*, 1440–1448.

Lu, W., Cheng, Y.C., Chen, K., Wang, H., Gerhard, G.S., Still, C.D., Chu, X., Yang, R., Parihar, A., O'Connell, J.R., et al. (2015). Evidence for several independent genetic variants affecting lipoprotein (a) cholesterol levels. Hum. Mol. Genet. *24*, 2390–2400.

Lundmark, R., Doherty, G.J., Howes, M.T., Cortese, K., Vallis, Y., Parton, R.G., and McMahon, H.T. (2008). The GTPase-Activating Protein GRAF1 Regulates the CLIC/GEEC Endocytic Pathway. Curr. Biol. *18*, 1802–1808.

Mack, S., Coassin, S., Rueedi, R., Yousri, N.A., Seppälä, I., Gieger, C., Schönherr, S., Forer, L., Erhart, G., Marques-Vidal, P., et al. (2017). A genome-wide association meta-analysis on lipoprotein (a) concentrations adjusted for apolipoprotein (a) isoforms. J. Lipid Res. *58*, 1834–1844.

Marques, P.E., Nyegaard, S., Collins, R.F., Troise, F., Freeman, S.A., Trimble, W.S., and Grinstein, S. (2019). Multimerization and Retention of the Scavenger Receptor SR-B1 in the Plasma Membrane. Dev. Cell *50*, 283-295.e5.

McCormick, S.P.A., and Schneider, W.J. (2019). Lipoprotein(a) catabolism: a case of multiple receptors. Pathology *51*, 155–164.

McIntyre, R.S., Soczynka, J.K., Konarski, J.Z., and Kennedy, S.H. (2006). The effect of antidepressants on lipid homeostasis: A cardiac safety concern? Expert Opin. Drug Saf. *5*, 523–537.

Miles, L.A., Andronicos, N.M., Baik, N., and Parmer, R.J. (2006). Cell-surface actin binds plasminogen and modulates neurotransmitter release from catecholaminergic cells. J. Neurosci. *26*, 13017–13024.

Miles, L.A., Lighvani, S., Baik, N., Andronicos, N.M., Chen, E.I., Parmer, C.M., Khaldoyanidi, S., Diggs, J.E., Kiosses, W.B., Kamps, M.P., et al. (2012). The Plasminogen Receptor , Plg-R KT , and Macrophage Function. *2012*.

Mooser, V., Seabra, M.C., Abedin, M., Landschulz, K.T., Marcovina, S., and Hobbs, H.H. (1996). Apolipoprotein(a) kringle 4-containing fragments in human urine: Relationship to plasma levels of lipoprotein(a). J. Clin. Invest. *97*, 858–864.

Morgan, B.M., Brown, A.N., Deo, N., Harrop, T.W.R., Taiaroa, G., Mace, P.D., Wilbanks, S.M., Merriman, T.R., Williams, M.J.A., and McCormick, S.P.A. (2020). Nonsynonymous SNPs in LPA homologous to plasminogen deficiency mutants represent novel null apo(a) alleles. J. Lipid Res. *61*, 432–444.

Otomo, M., Takahashi, K., Miyoshi, H., Osada, K., Nakashima, H., and Yamaguchi, N. (2008). Some selective serotonin reuptake inhibitors inhibit dynamin I guanosine triphosphatase (GTPase). Biol. Pharm. Bull. *31*, 1489–1495.

Pan, S. juan, Tan, Y. long, Yao, S. wu, Xin, Y., Yang, X., Liu, J., and Xiong, J. (2018). Fluoxetine induces lipid metabolism abnormalities by acting on the liver in patients and mice with depression. Acta Pharmacol. Sin. *39*, 1463–1472.

Paslakis, G., Kopf, D., Westphal, S., Gilles, M., Lederbogen, F., Hamann, B., Heuser, I., and Deuschle, M. (2011). Treatment with paroxetine, but not amitriptyline, lowers levels of lipoprotein(a) in patients with major depression. J. Psychopharmacol. *25*, 1344–1346.

Patel, A.P., Wang, M., Pirruccello, J.P., Ellinor, P.T., Ng, K., Kathiresan, S., and Khera, A. V. (2020). Lp(a) (Lipoprotein[a]) Concentrations and Incident Atherosclerotic Cardiovascular Disease. Arterioscler. Thromb. Vasc. Biol. 1–10.

Pellegrino, M., Furmaniak-kazmierczak, E., Leblanc, J.C., Cho, T., Cao, K., Marcovina, S.M., Boffa, M.B., and Co, G.P. (2004). The Apolipoprotein (a) Component of Lipoprotein (a) Stimulates Actin Stress Fiber Formation and Loss of Cell-Cell Contact in Cultured Endothelial Cells *. J. Biol. Chem. *279*, 6526–6533.

Rader, D.J., Mann, W.A., Cain, W., Kraft, H.G., Usher, D., Zech, L.A., Hoeg, J.M., Davignon, J., Lupien, P., Grossman, M., et al. (1995). The low density lipoprotein receptor is not required for normal catabolism of Lp(a) in humans. J. Clin. Invest. *95*, 1403–1408.

Rami, M., Guillamat-Prats, R., Rinne, P., Salvermoser, M., Ring, L., Bianchini, M., Blanchet, X., Megens, R.T.A., Döring, Y., Walzog, B., et al. (2018). Chronic intake of the selective serotonin reuptake inhibitor fluoxetine enhances atherosclerosis. Arterioscler. Thromb. Vasc. Biol. *38*, 1007–1019.

Reblin, T., Niemeier, A., Meyer, N., Willnow, T.E., Kronenberg, F., Dieplinger, H., Greten, H., and Beisiegel, U. (1997). Cellular uptake of lipoprotein[a] by mouse embryonic fibroblasts via the LDL receptor and the LDL receptor-related protein. J. Lipid Res. *38*, 2103–2110.

Redpath, G.M.I., Betzler, V.M., Rossatti, P., and Rossy, J. (2020). Membrane Heterogeneity Controls Cellular Endocytic Trafficking. Front. Cell Dev. Biol. *8*.

Reglero-Real, N., Álvarez-Varela, A., Cernuda-Morollón, E., Feito, J., Marcos-Ramiro, B., Fernández-Martín, L., Gómez-Lechón, M.J., Muntané, J., Sandoval, P., Majano, P.L., et al. (2014). Apicobasal polarity controls lymphocyte adhesion to hepatic epithelial cells. Cell Rep. *8*, 1879–1893.

Romagnuolo, R., Scipione, C.A., Marcovina, S.M., Gemin, M., Seidah, N.G., Boffa, M.B., and Koschinsky, M.L. (2017). Roles of the low density lipoprotein receptor and related receptors in inhibition of lipoprotein(a) internalization by proprotein convertase subtilisin/kexin type 9. PLoS One *12*, e0180869.

Sathe, M., Muthukrishnan, G., Rae, J., Disanza, A., Thattai, M., Scita, G., Parton, R.G., and Mayor, S. (2018). Small GTPases and BAR domain proteins regulate branched actin polymerisation for clathrin and dynamin-independent endocytosis. Nat. Commun. *9*, 1–16.

Schindelin, J., Arganda-Carreras, I., Frise, E., Kaynig, V., Longair, M., Pietzsch, T., Preibisch, S., Rueden, C., Saalfeld, S., Schmid, B., et al. (2012). Fiji: an open-source platform for biological-image analysis. Nat. Methods *9*, 676–682.

Sharma, M., Redpath, G.M., Williams, M.J.A., and McCormick, S.P.A. (2017). Recycling of Apolipoprotein(a) After PlgRKT-Mediated Endocytosis of Lipoprotein(a). Circ. Res. *120*, 1091–1102.

Tam, S.P., Zhang, X., and Koschinsky, M.L. (1996). Interaction of a recombinant form of apolipoprotein[a] with human fibroblasts and with the human hepatoma cell line HepG2. J. Lipid

Res. *37*, 518–533.

Traub, L.M., and Bonifacino, J.S. (2013). Cargo recognition in clathrin-mediated endocytosis. Cold Spring Harb. Perspect. Biol. *5*.

Wei, F., Crain, A.L., Whitebird, R.R., Godlevsky, O. V., and Oconnor, P.J. (2009). Effects of paroxetine and sertraline on low-density lipoprotein cholesterol: An observational cohort study. CNS Drugs *23*, 857–865.

Wilson, D.P., Jacobson, T.A., Jones, P.H., Koschinsky, M.L., McNeal, C.J., Nordestgaard, B.G., and Orringer, C.E. (2019). Use of Lipoprotein(a) in clinical practice: A biomarker whose time has come. A scientific statement from the National Lipid Association. J. Clin. Lipidol. *13*, 374–392.

Yang, X., Amar, M.J., Vaisman, B., Bocharov, A. V, Vishnyakova, T.G., Freeman, L.A., Kurlander, R.J., Patterson, A.P., Becker, L.C., and Remaley, A.T. (2013). Scavenger receptor-BI is a receptor for lipoprotein (a). J. Lipid Res. *54*, 2450–2457.

Zanoni, P., Velagapudi, S., Yalcinkaya, M., Rohrer, L., and von Eckardstein, A. (2018). Endocytosis of lipoproteins. Atherosclerosis *275*, 273–295.

Figure 1: Lp(a) uptake in liver cells is regulated by macropinocytosis. (A) Representative images of HepG2 cells incubated with Lp(a) for 1 hour following H_2O vehicle (left panel) or 2.5 mM EGTA (right panel) treatment for 1 hour. **(B)** Percentage of Lp(a) vesicles detected in EGTA treated cells compared to vehicle control. **(C)** Representative images of HepG2 cells incubated with Lp(a) for 1 hour following DMSO vehicle (left panel) or 50µM EIPA (right panel) treatment for 1 hour. **(D)** Percentage of Lp(a) vesicles detected in EIPA treated cells compared to vehicle control. **(E)** Representative images of HepG2 cells incubated with apo(a)-mScarlet for 1 hour following DMSO vehicle (left panel) or 50µM EIPA (right panel) treatment for 1 hour. **(F)** Percentage of apo(a)-mScarlet vesicles detected in EIPA treated cells compared to vehicle control. *= $p<0.05$, **= $p<0.01$ from one sample T-test comparing values to vehicle treated controls normalised to 100%. Data points represent means of independent experiments quantified from 5 fields of view of ~20 cells per field from each independent experiment. Error bars represent standard error of the mean. Lp(a) was detected using the α-LPA4 primary antibody and AlexaFluor conjugated anti-mouse secondary antibody. Apo(a)-mScarlet was directly detected. Images were acquired on an Olympus FV1000/FV1200 confocal microscope. Scale bar= 5 µM.

Figure 2: Lp(a) macropinocytosis is inhibited by antidepressants in macrophages. (A) Representative images of PMA-differentiated THP-1 cells incubated with Lp(a) for 1 hour following H_2O vehicle (left panel) or 2.5 mM EGTA (right panel) treatment for 1 hour. **(B)** Percentage of Lp(a) vesicles detected in EGTA treated cells compared to vehicle control. **(C)** Representative images of PMA-differentiated THP-1 cells incubated with Lp(a) for 1 hour following DMSO vehicle (left panel) or 1 mM amiloride (right panel) treatment for 1 hour. **(D)** Percentage of Lp(a) vesicles detected in amiloride treated cells compared to vehicle control. **(E)** Representative images of PMA-differentiated THP-1 cells incubated with Lp(a) for 1 hour following H_2O vehicle, 20 µM imipramine, 50 µM citalopram, 20 µM fluoxetine or 20 µM sertraline (left to right) treatment overnight. **(F)** Representative images of PMA-differentiated THP-1 cells incubated 70 kDa dextran-TRITC for 1 hour following H_2O vehicle or 20 µM imipramine, 50 µM citalopram, 20 µM fluoxetine or 20 µM sertraline (left to right) treatment overnight. **(G)** Percentage of Lp(a) vesicles detected in antidepressant treated cells compared to vehicle control. **(H)** Percentage of dextran-TRITC vesicles detected in antidepressant treated cells compared to vehicle control. n.s= not significant, *= $p<0.05$, **=$p<0.01$ from on sample t-test **(B)**, **(D)** or randomised block ANOVA **(G)**, **(H)** comparing treated cells to vehicle control. Data points represent means of independent experiments quantified from 5 fields of view of ~20 cells per field from each independent experiment. Error bars represent standard error of the mean. Lp(a) was detected using α-LPA4 primary antibody and AlexaFluor conjugated anti-mouse secondary antibody. 70 kDa dextran-TRITC was detected directly. Images were acquired on an Olympus FV1000/FV3000 confocal microscope. Scale bar= 5 µM.

Figure 3: Antidepressants have variable effects on Lp(a) uptake in liver cells. (A) Representative images of HepG2 cells incubated with Lp(a) for 1 hour following H_2O vehicle (left) or 20 µM imipramine (right panel) treatment overnight. **(B)** Percentage of Lp(a) vesicles detected following overnight treatment with 5, 10, and 20 µM imipramine compared to vehicle control. **(C)** Percentage of Lp(a) vesicles detected in 20 µM imipramine treated cells compared to vehicle control. **(D)** Representative images of HepG2 cells incubated with Lp(a) for 1 hour following H_2O vehicle (left) or 50 µM citalopram (right panel) treatment overnight. **(E)** Percentage of Lp(a) vesicles detected following overnight treatment with 5, 10, 20 and 50 µM citalopram compared to vehicle control. **(F)** Percentage of Lp(a) vesicles detected in 50 µM citalopram treated cells compared to vehicle control. **(G)** Representative images of HepG2 cells incubated with Lp(a) for 1 hour following H_2O vehicle (left) or 20 µM fluoxetine (right) for 2 hours. **(H)** Percentage of Lp(a) vesicles detected following 2 hours treatment with 5, 10, and 20 µM fluoxetine compared to vehicle control. **(I)** Percentage of Lp(a) vesicles detected in 20 µM fluoxetine treated cells compared to vehicle control. **(J)** Representative images of HepG2 cells incubated with Lp(a) for 1 hour following H_2O vehicle (left) or 20 µM sertraline (right) for 2 hours. **(K)** Percentage of Lp(a) vesicles detected following 2 hours treatment with 5, 10, and 20 µM sertraline compared to vehicle control. **(L)** Percentage of Lp(a) vesicles detected in 20 µM sertraline treated cells compared to vehicle control. **(M)** Representative images of HepG2 cells incubated with 70kDa dextran-TRITC for 1 hour following H_2O vehicle (left to right), 20 µM imipramine (overnight), 50 µM citalopram (overnight), 20 µM fluoxetine (2 hours) and 20 µM sertraline (2 hours) treatment. **(N)** Percentage of 70 kDa dextran-TRITC vesicles detected following treatment with antidepressants compared to vehicle control. n.s. = not significant, *= $p<0.05$, **=$p<0.01$ from one sample T-test comparing values to vehicle treated controls normalised to 100% **(I)**, **(L)**, Wilcoxon rank sum test **(C, F)** or randomised-block ANOVA **(N)**. Data points represent means of independent experiments quantified from 5 fields of view of ~20 cells per field from each independent experiment. Error bars represent standard error of the mean. Lp(a) was detected using α-LPA4 primary antibody and AlexaFluor conjugated anti-mouse secondary antibody. Images were acquired on an Olympus FV1000/FV1200 confocal microscope. Scale bar= 5 µM.

Figure 4: Antidepressants specifically increase Lp(a) surface binding in liver cells. (A) Representative images of maximum z-projections of surface-bound Lp(a) following H_2O vehicle, 20 µM imipramine or 50 µM citalopram treatment overnight. **(B)** Percentage surface Lp(a) signal in imipramine and citalopram treated cells compared to vehicle control. **(C)** Representative images of maximum z-projections of surface-bound dextran following H_2O vehicle, 20 µM imipramine or 50 µM citalopram treatment overnight. **(D)** Percentage surface dextran signal in imipramine and citalopram treated cells compared to vehicle control. **(E)** Representative SEM images of HepG2 cells incubated with H_2O vehicle or 50 µM citalopram overnight. **(F)** Quantification of membrane ruffling events per cell in vehicle and citalopram treated cells. n.s. = not significant, *= $p<0.05$, p=<0.01 from randomised block ANOVA comparing treated to vehicle control conditions **(B,D,F)**. Data points represent means of independent experiments quantified from 5 fields of view of ~20 cells per field from each independent experiment **(B,D,F)**. Data points represent single cells **(H)**. Error bars represent standard error of the mean. 70 kDa dextran-TRITC was detected directly. Images were acquired on an Olympus FV1000/FV1200 confocal microscope **(A,C,E)** or an FEI Nova NanoSEM **(G).** Scale bar= 5 µM **(A,C,E)** or 2 µM **(G)**.

Figure 5: Imipramine and citalopram enhance Lp(a) delivery to Rab11$^+$ recycling endosomes. (A) Representative images of HepG2 cells incubated with Lp(a) for 30 minutes following H_2O vehicle (top panel), 20 µM imipramine (middle panel) or 50 µM citalopram (bottom panel) overnight. Cells were co-stained with anti-LPA4 (magenta) and anti-Rab11 (green) and detected with AlexaFluor secondary antibodies. **(B)** Representative images of HepG2 cells incubated with Lp(a) for 120 minutes following H_2O vehicle (top panel), 20 µM imipramine (middle panel) or 50 µM citalopram (bottom panel) overnight. Cells were co-stained with anti-LPA4 (magenta) and anti-Rab11 (green). **(C)** Representative images of HepG2 cells incubated with Lp(a) for 30 minutes following H_2O vehicle (top panel), 20 µM imipramine (middle panel) or 50 µM citalopram (bottom panel) overnight. Cells were co-stained with anti-LPA4 (magenta) and anti-Rab7 (green) and detected with AlexaFluor secondary antibodies. **(D)** Representative images of HepG2 cells incubated with Lp(a) for 120 minutes following H_2O vehicle (top panel), 20 µM imipramine (middle panel) or 50 µM citalopram (bottom panel) overnight. Cells were co-stained with anti-LPA4 (magenta) and anti-Rab7 (green). **(E)** Quantification of percentage vesicle overlap between Lp(a) and Rab11 channels. **(F)** Quantification of percentage vesicle overlap between Lp(a) and Rab7 channels. n.s.= not significant, *= $p<0.05$, **= $p<0.01$ from randomised block ANOVA comparing treated to vehicle control conditions at each timepoint. Data points represent means of independent experiments quantified from 5 fields of view of ~20 cells per field from each independent experiment. Error bars represent standard error of the mean. Images were acquired on an Olympus FV1000/FV1200 confocal microscope. Scale bar= 5 µM.

Figure 6: Imipramine and citalopram stimulate Lp(a) and apo(a) recycling. (A) Representative Western blots of HepG2 cells treated with vehicle (H_2O), 20 µM imipramine or 50 µM citalopram and incubated with Lp(a) for 2 hours, after which Lp(a) containing media was removed and replaced with fresh Lp(a)-free media and lysates collected immediately or after 2 or 6 hours (labelled 0, 2 and 6 hr, respectively). **(B)** Quantification of Lp(a) band intensity normalised to actin band intensity at 0, 2 and 6 hours with vehicle, imipramine or citalopram treatment. **(C)** Representative Western blots of Lp(a) immunoprecipitated from fresh cell media collected 0, 2 or 6 hours after vehicle, imipramine or citalopram treated HepG2 were incubated with Lp(a) for 2 hours in **(A)**. **(D)** Quantification of total immunoprecipitated Lp(a) band intensity 2- and 6-hours following removal of Lp(a) containing media. **(E)** Representative Western blots of HepG2 cells treated with vehicle (H_2O), 20 µM imipramine or 50 µM citalopram and incubated with apo(a)-mScarlet/tGFP for 2 hours, after which apo(a)-mScarlet/tGFP containing media was removed and replaced with fresh apo(a)-mScarlet/tGFP-free media and lysates collected immediately or after 2 or 6 hours (labelled 0, 2 and 6 hr, respectively). **(F)** Quantification of apo(a)-mScarlet/tGFP band intensity normalised to actin band intensity at 0, 2 and 6 hours with vehicle, imipramine or citalopram treatment. **(G)** Representative Western blots of apo(a)-mScarlet/tGFP immunoprecipitated from fresh cell media collected 0, 2 or 6 hours after vehicle, imipramine or citalopram treated HepG2 were incubated with apo(a)-mScarlet/tGFP for 2 hours in **(E)**. **(H)** Quantification of total immunoprecipitated apo(a)-mScarlet/tGFP band intensity 2- and 6-hours following removal of apo(a)-mScarlet/tGFP containing media. n.s.= not significant, *= $p<0.05$, **= $p<0.01$ from randomised block ANOVA. Data points represent means of independent experiments. Error bars represent standard error of the mean.

Figure 7: Summary of the effects of antidepressants on Lp(a) uptake and subcellular trafficking in liver cells. **(1)** Imipramine and citalopram enhance Lp(a) binding to the cell surface, resulting in increased Lp(a) engulfment by macropinocytosis. **(2)** Sertraline inhibits Lp(a) uptake via macropinocytosis into the cell. **(3)** Imipramine and citalopram increase the sorting of Lp(a) into Rab11-positive recycling endosomes, but not Rab7 or LAMP1 positive compartments. **(4)** As a consequence of increased delivery into Rab11-postive recycling endosomes, imipramine and citalopram lead to increased recycling of apo(a) back into the cellular media.

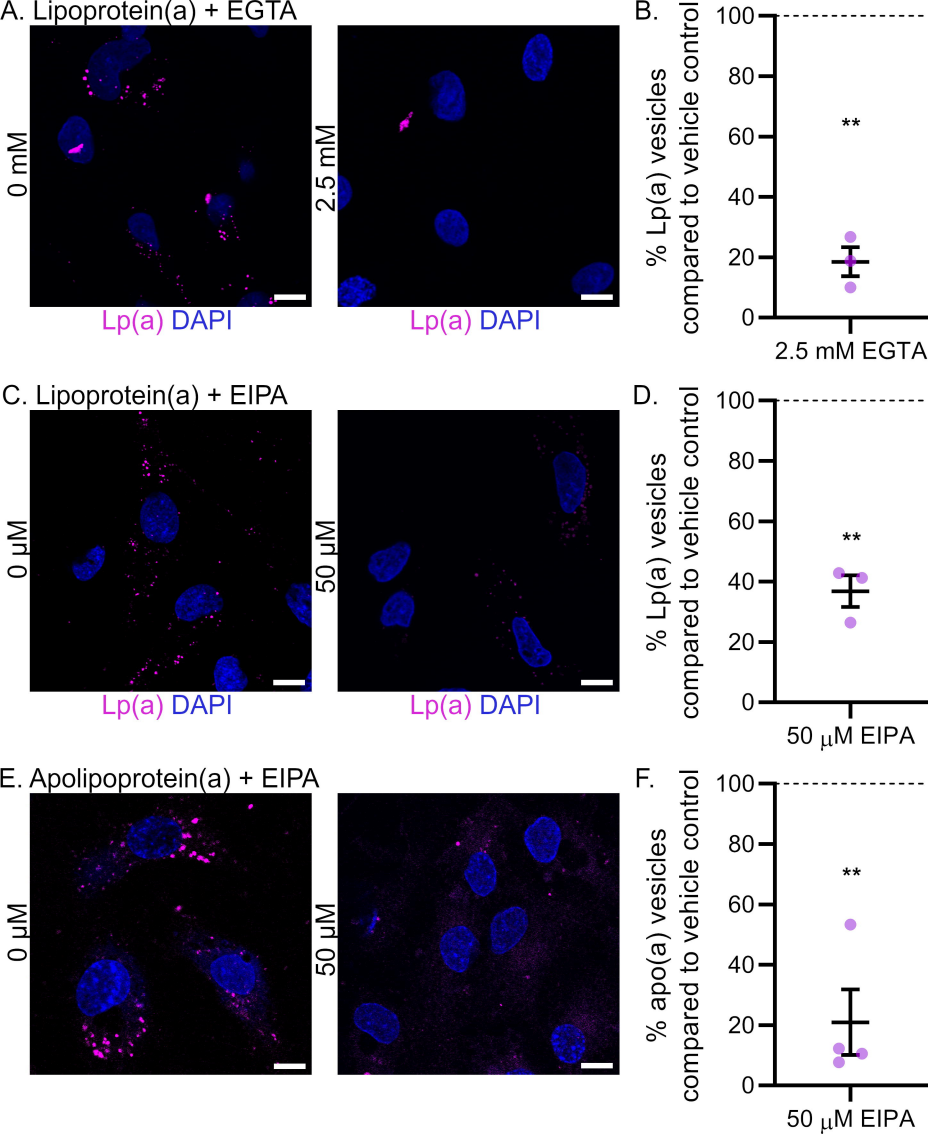
A. Lipoprotein(a) + EGTA
0 mM
2.5 mM
Lp(a) DAPI
Lp(a) DAPI
B.
% Lp(a) vesicles compared to vehicle control
100
80
60
40
20
0
**
2.5 mM EGTA
C. Lipoprotein(a) + EIPA
0 μM
50 μM
Lp(a) DAPI
Lp(a) DAPI
D.
% Lp(a) vesicles compared to vehicle control
100
80
60
40
20
0
**
50 μM EIPA
E. Apolipoprotein(a) + EIPA
0 μM
50 μM
F.
% apo(a) vesicles compared to vehicle control
100
80
60
40
20
0
**
50 μM EIPA

A. Lipoprotein(a) + EGTA

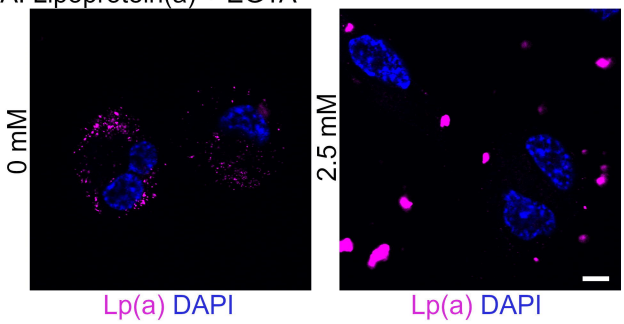

B.

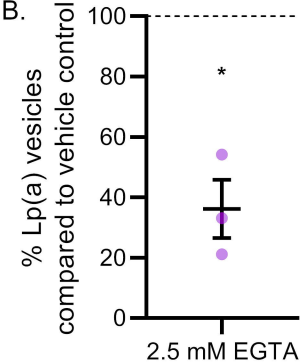

C. Lipoprotein(a) + Amiloride

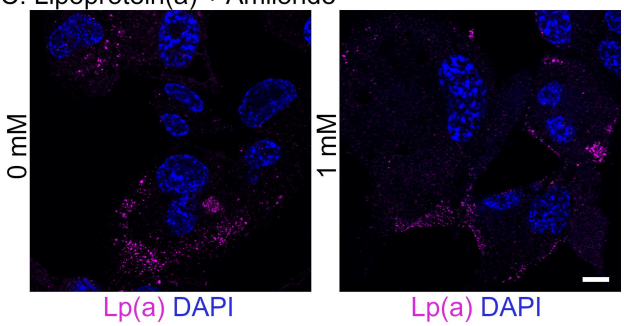

D.

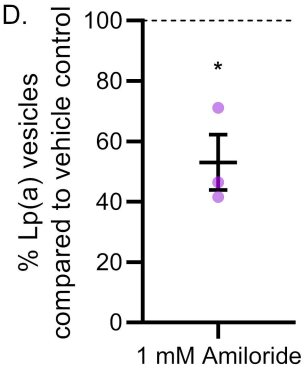

E. Lipoprotein(a) + antidepressants

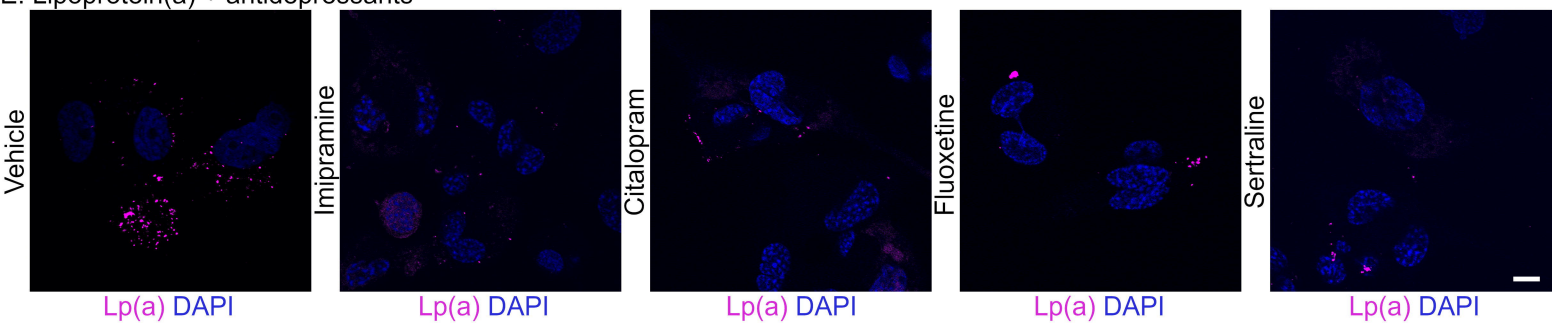

F. Dextran + antidepressants

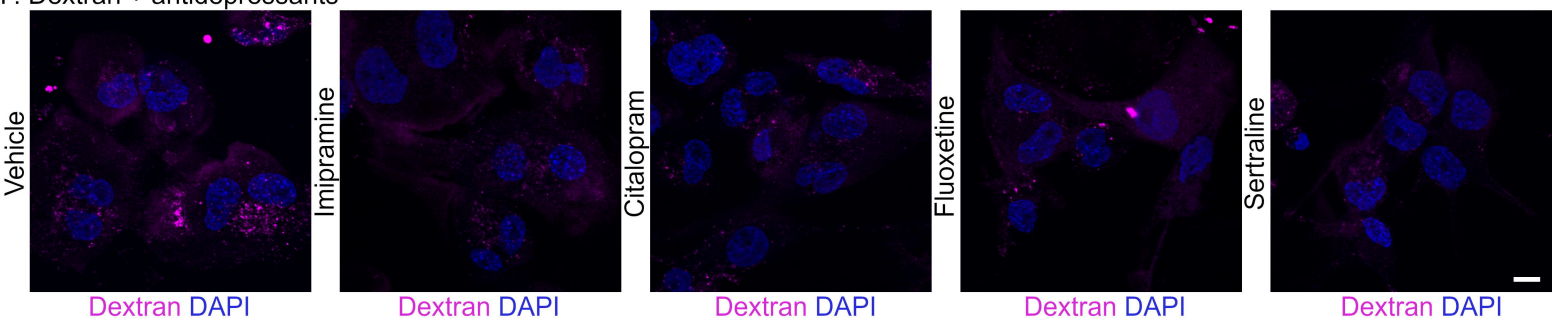

G.

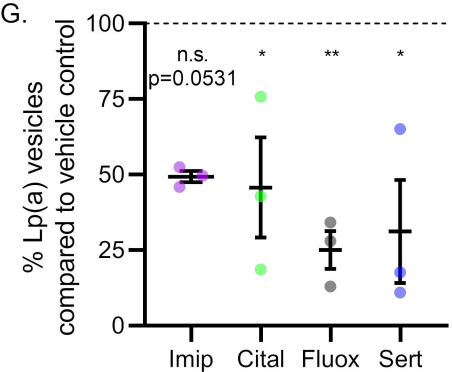

H.

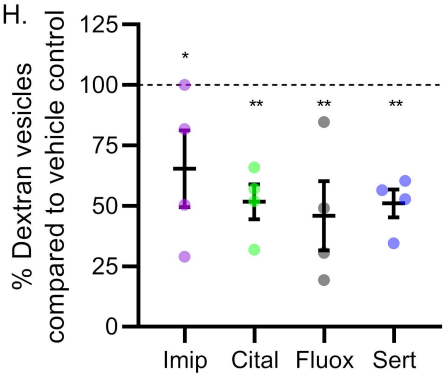

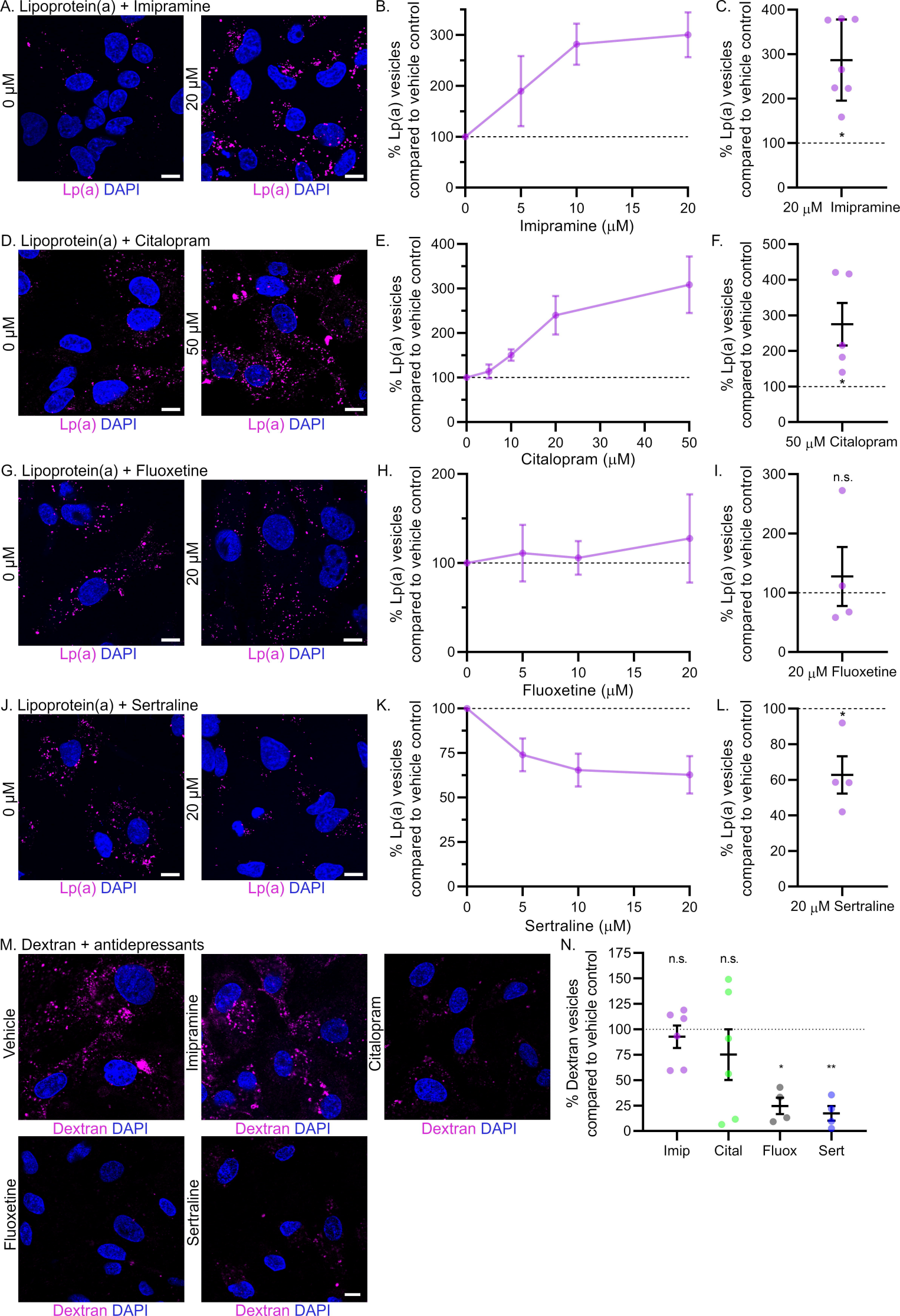
A. Lipoprotein(a) + Imipramine
0 μM
20 μM
Lp(a) DAPI
Lp(a) DAPI
B.
% Lp(a) vesicles compared to vehicle control
Imipramine (μM)
C.
20 μM Imipramine
D. Lipoprotein(a) + Citalopram
0 μM
50 μM
E.
Citalopram (μM)
F.
50 μM Citalopram
G. Lipoprotein(a) + Fluoxetine
0 μM
20 μM
H.
Fluoxetine (μM)
I.
n.s.
20 μM Fluoxetine
J. Lipoprotein(a) + Sertraline
0 μM
20 μM
K.
Sertraline (μM)
L.
20 μM Sertraline
M. Dextran + antidepressants
Vehicle
Imipramine
Citalopram
Fluoxetine
Sertraline
Dextran DAPI
N.
% Dextran vesicles compared to vehicle control
n.s.
n.s.
Imip
Cital
Fluox
Sert

A. Surface Lp(a)

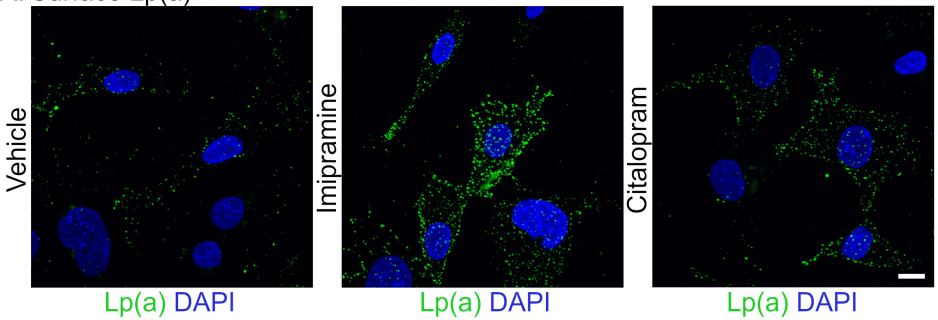

B.

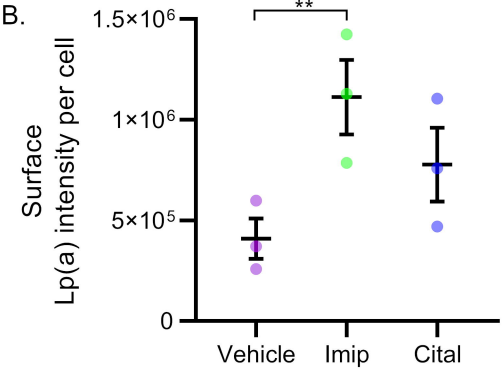

C. Surface Dextran-TRITC

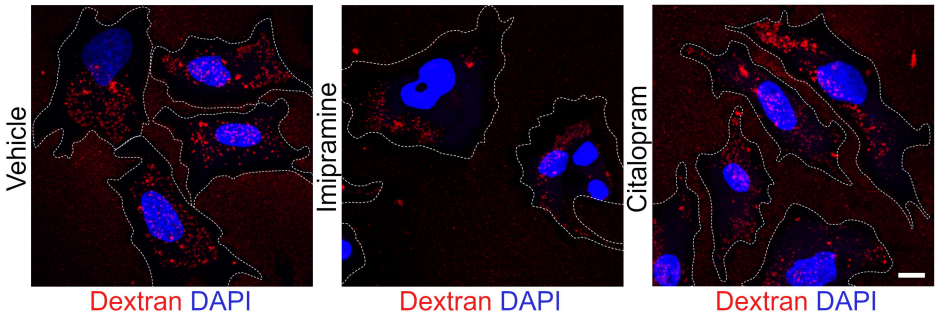

D.

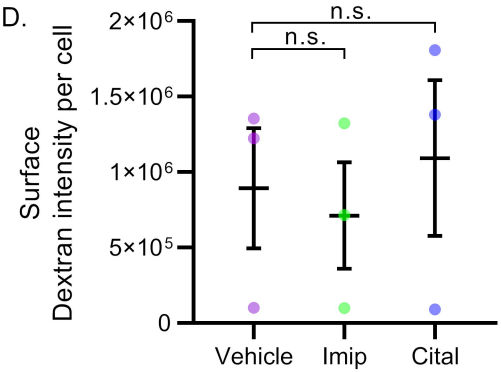

E. Vehicle

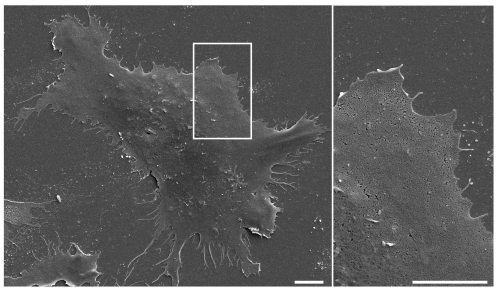

Citalopram

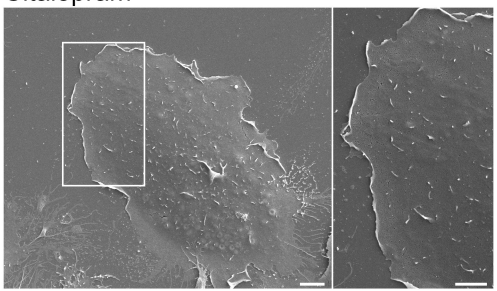

F.

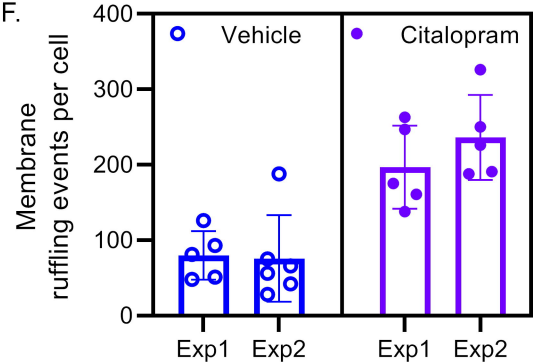

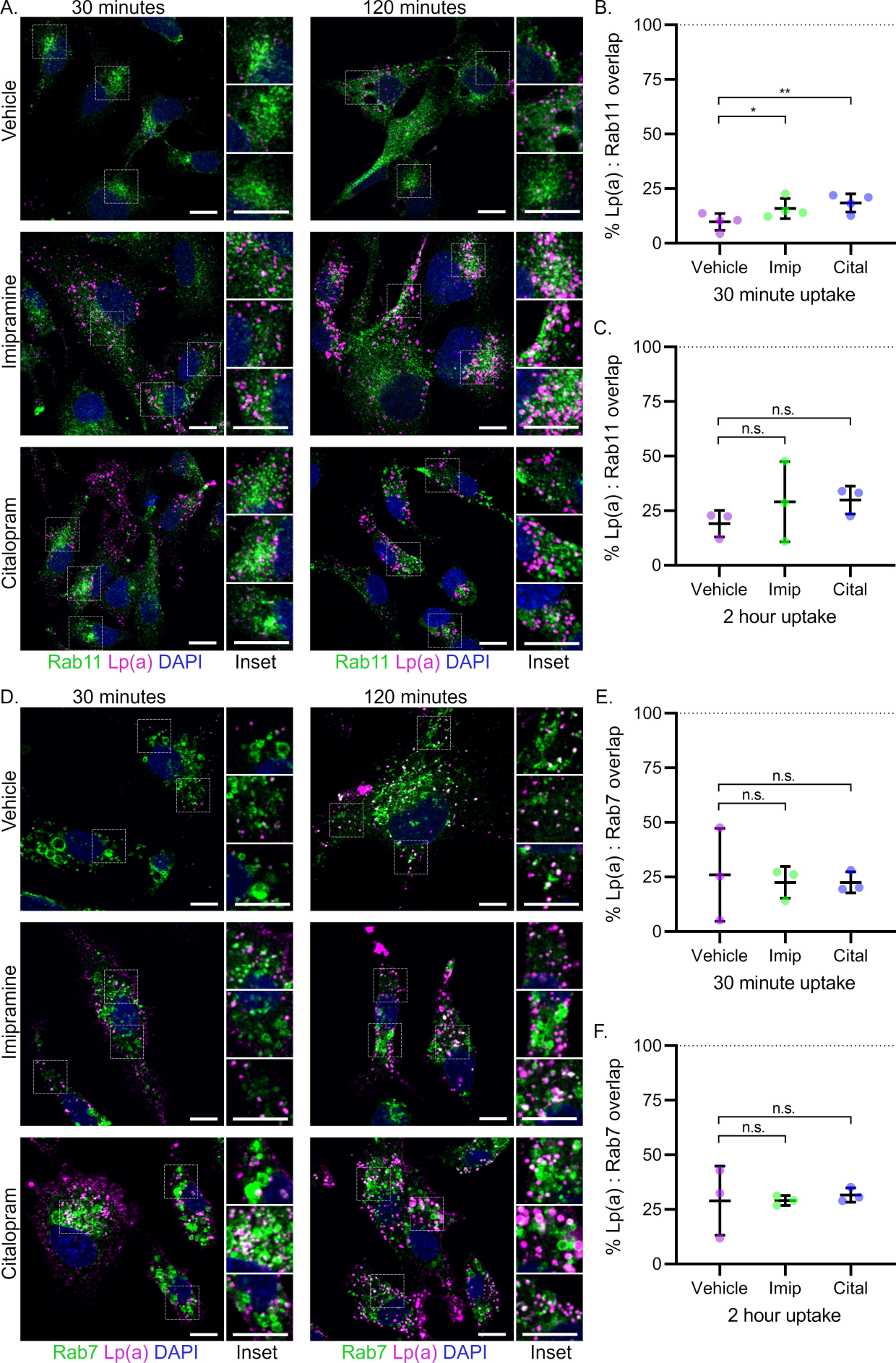
A.
30 minutes
120 minutes
Vehicle
Imipramine
Citalopram
Rab11 Lp(a) DAPI
Inset
Rab11 Lp(a) DAPI
Inset
B.
% Lp(a) : Rab11 overlap
100
75
50
25
0
*
**
Vehicle
Imip
Cital
30 minute uptake
C.
% Lp(a) : Rab11 overlap
n.s.
n.s.
Vehicle
Imip
Cital
2 hour uptake
D.
30 minutes
120 minutes
Vehicle
Imipramine
Citalopram
Rab7 Lp(a) DAPI
Inset
Rab7 Lp(a) DAPI
Inset
E.
% Lp(a) : Rab7 overlap
n.s.
n.s.
Vehicle
Imip
Cital
30 minute uptake
F.
% Lp(a) : Rab7 overlap
n.s.
n.s.
Vehicle
Imip
Cital
2 hour uptake

A. Internalised Lp(a)

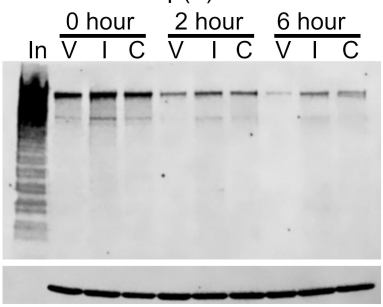

B.

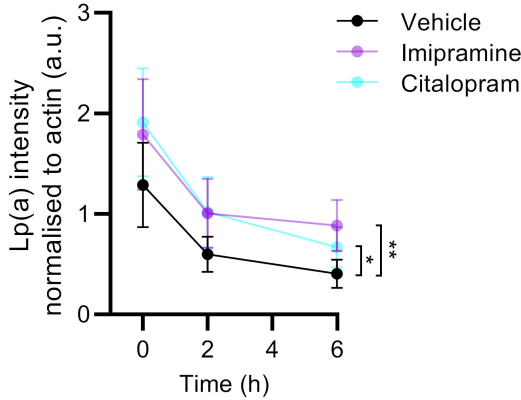

C. Recycled Lp(a)

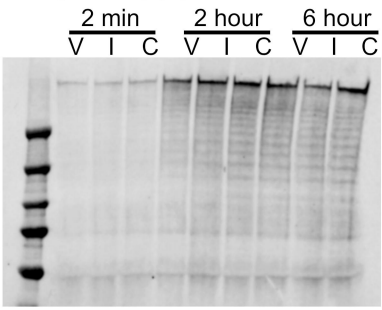

D.

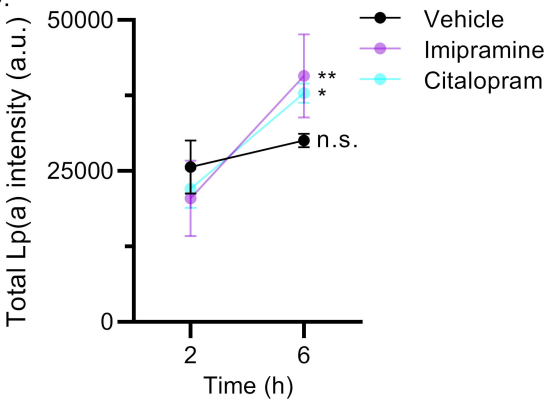

E. Internalised apo(a)

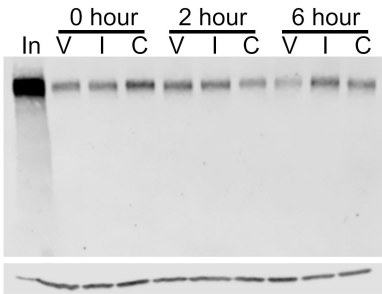

F.

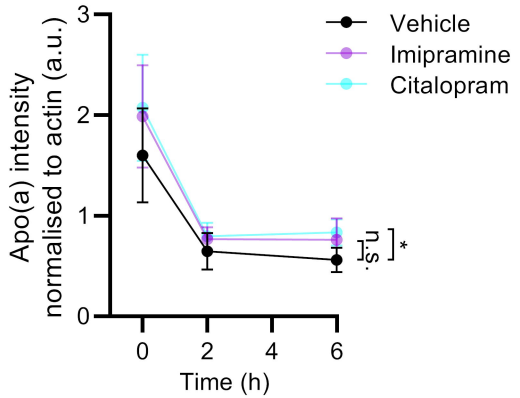

G. Recycled apo(a)

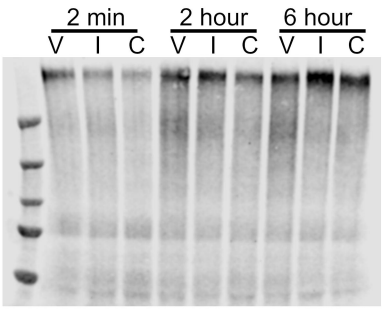

H.

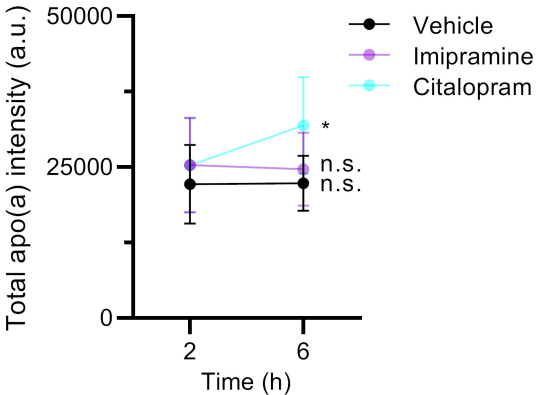

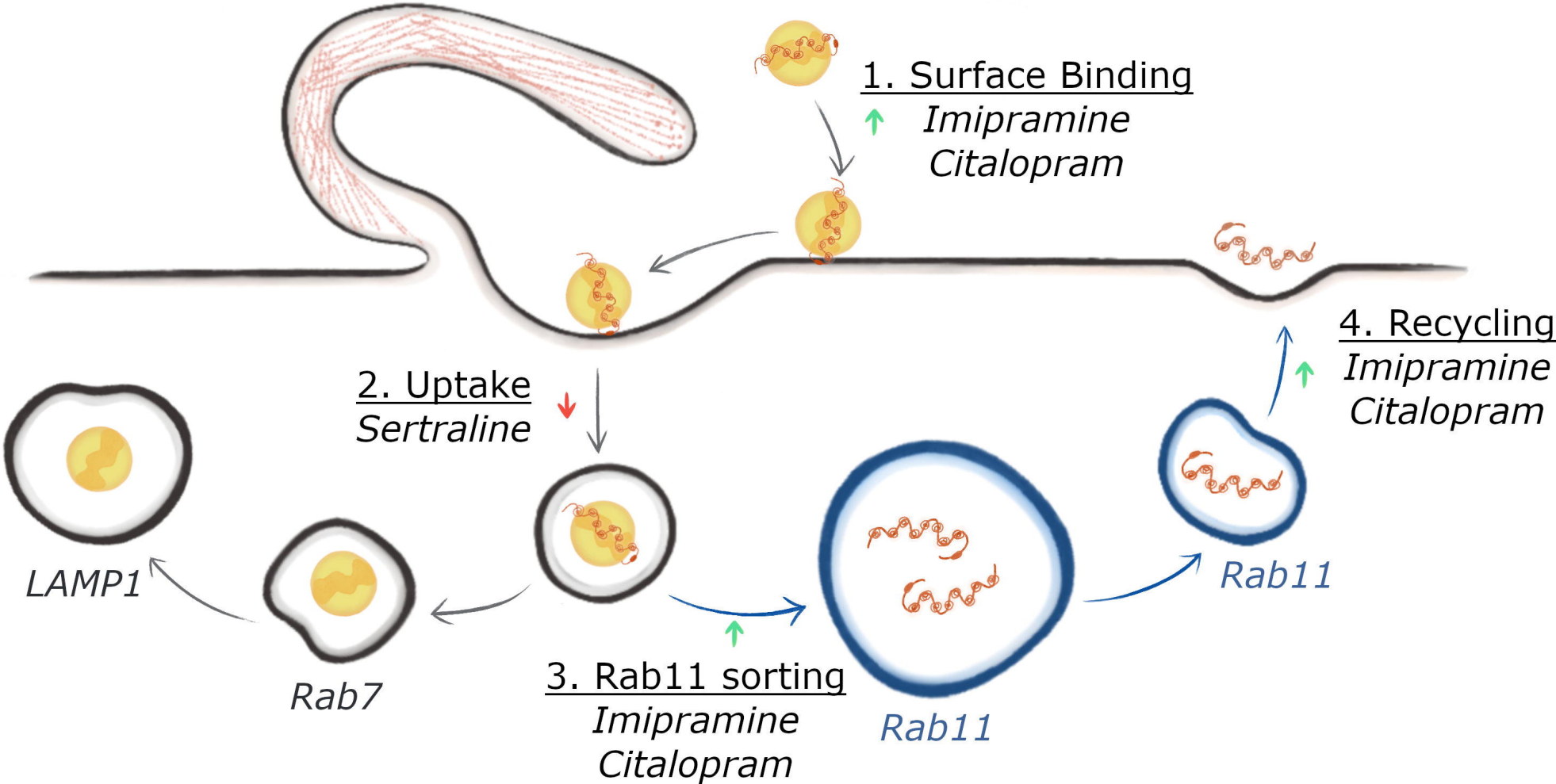
1. Surface Binding
Imipramine
Citalopram
2. Uptake
Sertraline
3. Rab11 sorting
Imipramine
Citalopram
4. Recycling
Imipramine
Citalopram
LAMP1
Rab7
Rab11
Rab11